IBRO Reports 4 (2018) 22–37

Contents lists available at ScienceDirect

IBRO Reports

journal homepage: http://www.journals.elsevier.com/ibro-reports

Research Paper

Expression of aggrecan components in perineuronal nets in the mouse cerebral cortex

Hiroshi Ueno[a,b,c,*], Kazuki Fujii[c,d], Shunsuke Suemitsu[e], Shinji Murakami[e], Naoya Kitamura[e], Kenta Wani[e], Shozo Aoki[e], Motoi Okamoto[b], Takeshi Ishihara[e], Keizo Takao[c,d]

[a] Department of Medical Technology, Kawasaki University of Medical Welfare, Okayama, 701-0193, Japan
[b] Department of Medical Technology, Graduate School of Health Sciences, Okayama University, Okayama, 700-8558, Japan
[c] Life Science Research Center, University of Toyama, Toyama, 930-0194, Japan
[d] Department of Behavioral Physiology, Graduate School of Innovative Life Science, University of Toyama, Toyama, 930-0194, Japan
[e] Department of Psychiatry, Kawasaki Medical School, Okayama, 701-0192, Japan

ARTICLE INFO

Article history:
Received 2 September 2017
Accepted 27 January 2018

Keywords:
Aggrecan
Brain region-specific
Chondroitin sulfate proteoglycan
Extracellular matrix
Perineuronal nets
Plasticity

ABSTRACT

Specific regions of the cerebral cortex are highly plastic in an organism's lifetime. It is thought that perineuronal nets (PNNs) regulate plasticity, but labeling for Wisteria floribunda agglutinin (WFA), which is widely used to detect PNNs, is observed throughout the cortex. The aggrecan molecule—a PNN component—may regulate plasticity, and may also be involved in determining region-specific vulnerability to stress. To clarify cortical region-specific plasticity and vulnerability, we qualitatively analyzed aggrecan-positive and glycosylated aggrecan-positive PNNs in the mature mouse cerebral cortex. Our findings revealed the selective expression of both aggrecan-positive and glycosylated aggrecan-positive PNNs in the cortex. WFA-positive PNNs expressed aggrecan in a region-specific manner in the cortex. Furthermore, we observed variable distributions of PNNs containing WFA- and aggrecan-positive molecules. Together, our findings suggest that PNN components and their function differ depending on the cortical region, and that aggrecan molecules may be involved in determining region-specific plasticity and vulnerability in the cortex.

1. Introduction

To preserve region-specific functions, certain areas of the cortex are associated with high and low plasticity over the course of development (Craig and Commins, 2006; Kolb, 2009). One molecule that is crucial in maintaining cortical plasticity is the perineuronal net (PNN), a highly condensed extracellular matrix (ECM) molecule in the central nervous system (Sorg et al., 2016). The PNN is a mesh-like structure that surrounds the cell body, proximal dendrites, and axonal initial segment of specific neurons. Approximately 15% of neurons in the mature brain are surrounded by PNNs (Guimarães et al., 1990; McRae et al., 2007), most of which are parvalbumin (PV)-positive GABAergic interneurons, and a small portion of which are pyramidal cells (Härtig et al., 1994; Wegner et al., 2003).

Maturation of GABAergic circuitry in the sensory cortex implies the onset of a critical period that is associated with cortical plasticity (Hensch and Fagiolini, 2005; Maffei and Turrigiano, 2008). The formation of PNNs around PV-positive interneurons in the sensory cortex indicates the end of this so-called critical period (Pizzorusso et al., 2002; McRae et al., 2007). In the visual cortex of

Abbreviations: FrA, frontal association cortex; DLO, dorsolateral orbital cortex; LO, lateral orbital cortex; VO, ventral orbital cortex; Cg, cingulate cortex; PL, prelimbic cortex; IL, infralimbic cortex; DP, dorsal peduncular cortex; M1, primary motor cortex; M2, secondary motor cortex; MPtA, medial parietal association cortex; LPtA, lateral parietal association cortex; S1Tr, primary somatosensory cortex–trunk region; S1BF, primary somatosensory cortex–barrel field; S2, secondary somatosensory cortex; V2MM, secondary visual cortex–mediomedial area; V2ML, secondary visual cortex mediolateral area; V1M, primary visual cortex monocular area; V1B, primary visual cortex binocular area; V2L, secondary visual cortex lateral area; Au1, primary auditory cortex; AuD, secondary auditory cortex dorsal area; AuV, secondary auditory cortex ventral area; TeA, temporal association cortex; Ect, ectorhinal cortex; PRh, perirhinal cortex; DIEnt, dorsintermed entorhinal cortex; DLEnt, dorsolateral entorhinal cortex; RSD, retrosplenial dysgranular cortex; RSGc, retrosplenial granular cortex c region; RSGb, retrosplenial granular cortex b region; RSGa, retrosplenial granular cortex a region.

* Corresponding author at: Department of Medical Technology, Kawasaki University of Medical Welfare, 288, Matsushima, Kurashiki, Okayama, 701-0193, Japan.
E-mail addresses: dhe422007@s.okayama-u.ac.jp (H. Ueno), kfujii@cts.u-toyama.ac.jp (K. Fujii), ssue@med.kawasaki-m.ac.jp (S. Suemitsu), muraka@med.kawasaki-m.ac.jp (S. Murakami), n-kitamura@med.kawasaki-m.ac.jp (N. Kitamura), kenta99101@yahoo.co.jp (K. Wani), shoaoki@med.kawasaki-m.ac.jp (S. Aoki), mokamoto@md.okayama-u.ac.jp (M. Okamoto), t-ishihara@med.kawasaki-m.ac.jp (T. Ishihara), takao@cts.u-toyama.ac.jp (K. Takao).

https://doi.org/10.1016/j.ibror.2018.01.002

the mature brain, it has been shown that treatment of PNNs with the enzyme, chondroitinase ABC, can restore plasticity (Pizzorusso et al., 2002). Similar mechanisms have been described for sensory input-dependent plasticity in other brain regions (Balmer et al., 2009; Gogolla et al., 2009).

Although the detailed function of PNNs is not clear, it is thought that their main roles involve neural plasticity, synaptic stability, and neuroprotective function (Sorg et al., 2016). The main constituents of PNNs include hyaluronic acid, tenascin-R, and the lectican family of chondroitin sulfate proteoglycans (CSPGs) (i.e., aggrecan, versican, brevican, and neurocan) (Bandtlow and Zimmermann, 2000; Yamaguchi, 2000). The plant-derived lectin, *Wisteria floribunda agglutinin* (WFA), has been widely used to detect PNNs through binding of *N*-acetylgalactosamine (Brückner et al., 1993; Schweizer et al., 1993; Seeger et al., 1994; Giamanco et al., 2010). Another method used to detect PNNs is through antibodies against aggrecan, the main PNN component (Matthews et al., 2002). These antibodies include AB1031 and Cat-315, with the former recognizing the central protein domain of the chondroitin sulfate glycosaminoglycan binding region of aggrecan (Giamanco et al., 2010; Lendvai et al., 2013), and the latter recognizing the HNK-1 carbohydrate epitope of aggrecan (Matthews et al., 2002; Dino et al., 2006; McRae et al., 2007).

While there is general agreement that PNNs regulate plasticity, WFA-labeled PNNs have been found throughout the cortex of the mature mouse (Brückner et al., 2000; Horii-Hayashi et al., 2015). Moreover, WFA-positive PNN labeling does not appear to vary over development (Horii-Hayashi et al., 2015). Considering that the plasticity of specific brain regions is highly variable over the span of an organism's lifetime, it is unlikely that WFA-positive PNNs control plasticity. Some studies have suggested the possibility that aggrecan molecules regulate plasticity as, during postnatal development, aggrecan expression is delayed when sensory input is deprived (McRae et al., 2007; Ye and Miao, 2013; Ueno et al., 2017b). Furthermore, when mice are housed in enriched environments after experimental cerebral ischemia, Cat-315-positive PNNs decrease (Madinier et al., 2014). In fact, it has been suggested that aggrecan molecules are not ubiquitously expressed throughout the cortex (Morawski et al., 2012a, 2012b; Ueno et al., 2017a). However, a quantitative analysis of aggrecan-positive PNNs in the cortex has not been conducted.

Along with their possible role in developmental plasticity, it has been suggested that aggrecan molecules are necessary for mediating the neuroprotective function of PNNs (Suttkus et al., 2014). It is well-established that certain brain regions are more susceptible to damage in neuropsychiatric disorders and neurodegenerative diseases. Interestingly, postmortem studies of patients with schizophrenia and autism show selective PNN abnormalities in the prefrontal and entorhinal cortices (Pantazopoulos et al., 2010; Mauney et al., 2013; Berretta et al., 2015). One theory explaining the cause of neuropsychiatric disorders is oxidative stress, which aggrecan-positive PNNs show resistance to (Gawryluk et al., 2011; Cabungcal et al., 2013; Suttkus et al., 2014). Indeed, in Alzheimer's disease, aggrecan-expressing PNNs are less susceptible to tau protein-induced damage (Morawski et al., 2010). It is therefore possible that aggrecan molecules are involved in neurological disorders, which target specific brain regions.

In this study, we focused on the quantitative measurement of aggrecan-positive PNNs and glycosylated aggrecan-positive PNNs in the mature mouse cortex. We examined the region-specific presence of aggrecan using three antibodies (i.e., AB1031, Cat-315, and Cat-316) that recognize different components of the aggrecan molecule (McRae et al., 2007, 2010; Foster et al., 2014; Madinier et al., 2014; Suttkus et al., 2014; Carstens et al., 2016; Morikawa et al., 2017). Note that Cat-316 recognizes the *o*-linked chondroitin sulfate epitope of aggrecan (Lander et al., 1997; Matthews et al., 2002). We believe that our findings will contribute to clarifying the state of region-selective vulnerability and plasticity in the cortex of individuals with neuropsychiatric disorders.

2. Materials and methods

2.1. Animals

Five adult male mice (C57BL/6J) were used for these experiments. Animals were purchased from Charles River Laboratories (Kanagawa, Japan), and housed in cages (3–5 animals per cage) with food and water available *ad libitum* under a 12 h light/dark cycle at 23–26 °C. All efforts were made to minimize the number of animals used and their suffering. All experimental protocols were performed in accordance with the U.S. National Institute of Health (NIH) Guide for the Care and Use of Laboratory Animals (NIH Publication No. 80-23, revised in 1996), and were approved by the Committee for Animal Experiments at Kawasaki Medical School Advanced Research Center and the Institutional Animal Care and Use Committee of University of Toyama.

2.2. Tissue preparation

For tissue preparation, animals were deeply anesthetized with a lethal dose of sodium pentobarbital (120 mg/kg, i.p.), and transcardially perfused, first with ice-cold phosphate buffered saline (PBS) for 2 min and then with 4% paraformaldehyde in PBS (pH 7.4) for 10 min (10 ml/min). Brains were dissected and postfixed overnight with 4% paraformaldehyde in PBS at 4 °C, and cryoprotected by immersion in 15% sucrose for 12 h followed by 30% sucrose for 20 h at 4 °C. Brains were frozen in O.C.T. Compound (Tissue-Tek; Sakuma Finetek, Tokyo, Japan) using dry ice-cold normal hexane, and serial coronal sections of 40-μm thickness were prepared using a cryostat (CM3050S; Leica Wetzlar, Germany) at −20 °C. Sections were collected in ice-cold PBS containing 0.05% sodium azide.

2.3. Immunohistochemistry

Cryostat sections were treated with 0.1% Triton X-100 in PBS at 20 °C for 15 min. After three washes in PBS, sections were incubated with 10% normal goat serum (ImmunoBioScience Corp, WA, USA) in PBS at room temperature for 1 h, washed three time in PBS, and incubated overnight at 4 °C in PBS containing biotinylated WFA (B-1355, Vector Laboratories, Funakoshi Co., Tokyo, Japan; 1:200) and primary antibodies (described below). After washing in PBS, sections were incubated with corresponding secondary antibodies (indicated below) and streptavidin-conjugated Texas Red (SA-5006, Vector Laboratories) at room temperature for 2 h. Labeled sections were rinsed again with PBS and mounted on glass slides with Vectashield medium (H-1400, Vector Laboratories). Prepared slides were either immediately imaged or stored at 4 °C.

2.4. Antibodies

The following primary antibodies were used for staining: rabbit anti-aggrecan (AB1031, Millipore, Tokyo, Japan; 1:200), mouse anti-aggrecan (Cat-315; MAB1581, Millipore, 1:1000), or mouse anti-aggrecan (Cat-316; MAB1582, Millipore, 1:10 000). The following secondary antibodies were used for visualization: Alexa Fluor 488-conjugated goat anti-rabbit IgG (ab150077, Abcam; Cambride, MA; 1:1000) or FITC-conjugated anti-mouse IgM (sc-2082, Santa Cruz, Texas, USA, 1:1000).

2.5. Microscopy imaging

For the quantification of WFA-, aggrecan-, Cat-315-, and Cat-316-positive PNNs, sections were stained as described previously

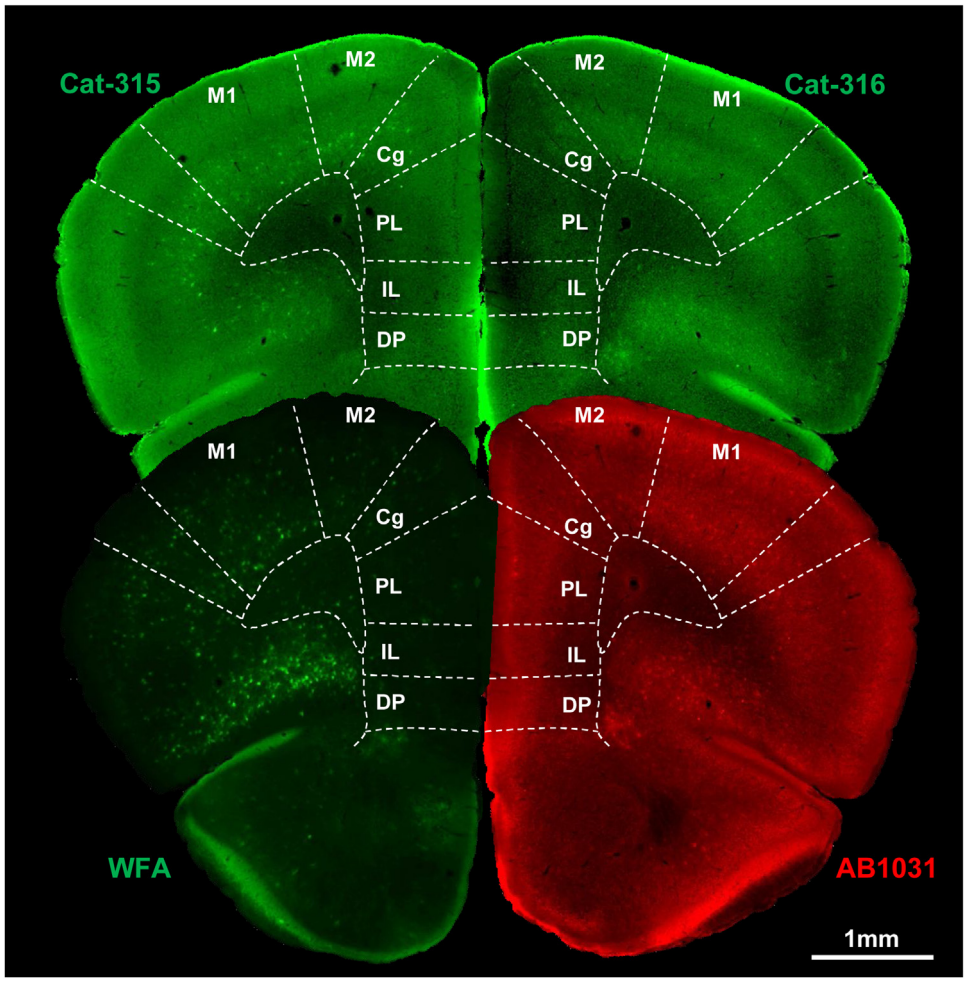

Fig. 1. Distribution of WFA-, AB1031-, Cat-315-, and Cat-316-positive PNNs in the mouse frontal cortex.
Representative whole brain sections labeled for WFA, AB1031, Cat-315, and Cat-316. Scale bar = 1 mm.

and imaged using confocal microscopy (LSM700; Carl Zeiss, Oberkochen, Germany). Images (1024 × 1024 pixel) were saved as TIFF files with ZEN software (Carl Zeiss). Briefly, low magnification analysis was performed using a 10 × objective lens, and a pinhole setting corresponding to a focal plane thickness of less than 1 μm. For observing PNN morphology, samples were randomly selected, and high-magnification images using a 100× objective lens were acquired. Images from whole sections were obtained using a 10× objective lens on a fluorescence microscope (BZ-X, KEYENCE, Tokyo, Japan), and merged using the KEYENCE BZ-X Analyzer software (KEYENCE).

2.6. Quantification of labeled PNNs

Brain regions were determined in accordance with the mouse brain atlas of Paxinos and Franklin (2012). From each mouse, 12 coronal sections were selected from the intermediate frontal, intermediate parietal, and rostral occipital cortices, and processed for staining. All confocal images were acquired as TIFF files, and analyzed with the NIH ImageJ software (NIH, Bethesda, MD, USA; http://rsb.info.nih.gov/nih-image/). The number of PNNs was quantified from at least three sections per region. Stained PNNs (soma size above 60 μm^2) were manually tagged and counted within the area of interest, and PNN density was calculated as cells/mm^2. Slides were coded and quantified by a blinded independent observer.

2.7. Data analysis

Data are expressed as the mean ± SEM of five animals. Statistical analyses were carried out using SPSS Statistics (IBM Corp., Armonk, NY, USA). Statistical significance was determined using a one-way analysis of variance (ANOVA) with post hoc tests, and statistical significance was set at $^{*}p < .05$.

3. Results

3.1. WFA-, AB1031-, Cat-315-, and Cat-316-positive PNNs in the mouse cerebral cortex

To examine PNN composition in the mouse cerebral cortex, we labeled PNNs with WFA lectin, as well as the following anti-aggrecan antibodies: AB1031, Cat-315, and Cat-316 (Figs. 1–3). Overall, we observed more WFA-positive (WFA+) PNNs in the mouse cerebral cortex than PNNs positive for AB1031, Cat-315, and Cat-316. While WFA+ PNNs appeared in many cortical areas, the expression of AB1031-, Cat-315-, and Cat-316-positive PNNs was area-specific. In general, we observed a greater number of labeled PNNs in the primary sensory cortices than in the association cortices and, as noted, the distribution of labeled PNNs was not homogenous across different areas or layers (Figs. 1–4). More specifically, a laminar pattern of labeling was observed in many cortical areas, with the most prominent and conspicuous labeling occurring in the mid-cortical layers and in layer I, respectively.

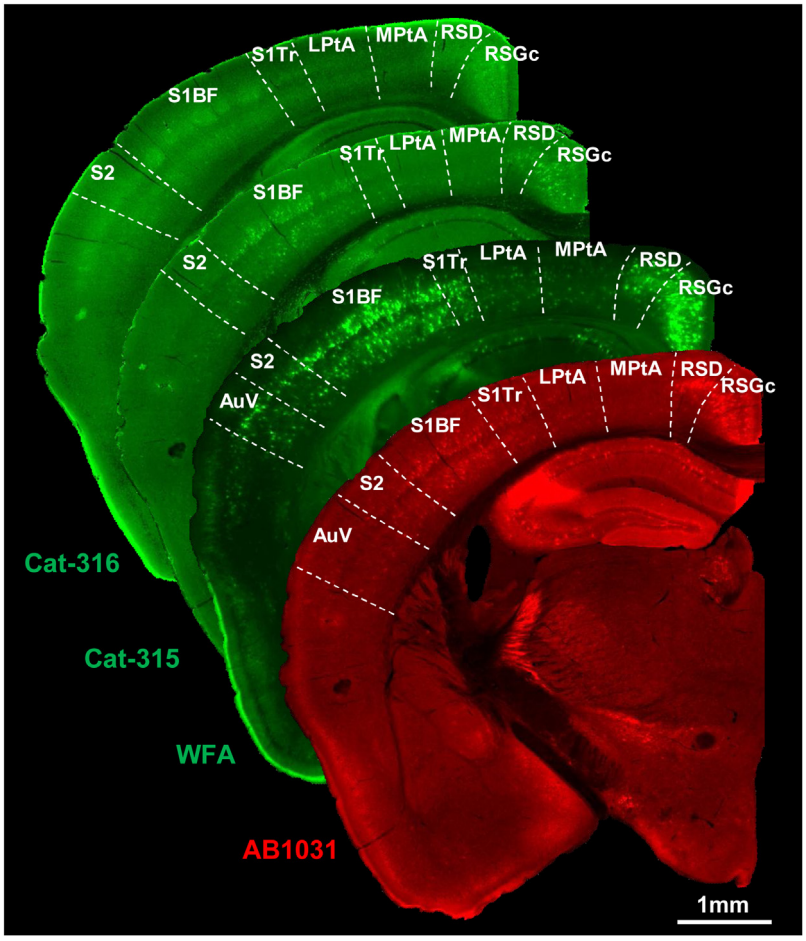

Fig. 2. Distribution of WFA-, AB1031-, Cat-315-, and Cat-316-positive PNNs in the mouse parietal cortex.
Representative whole brain sections labeled for WFA, AB1031, Cat-315, and Cat-316. Scale bar = 1 mm.

Taken together, these histochemical analyses revealed that the spatial expression of PNN components was region-specific.

3.2. Comparative distribution of WFA- and AB1031-positive PNNs

The density of WFA+ PNNs within the mouse cerebral cortex is shown in Fig. 5**A**. In the frontal cortex, low numbers of WFA+ PNNs were observed in the cingulate (Cg), prelimbic (PL), infralimbic (IL), and dorsal peduncular (DP) subregions. WFA+ PNNs were significantly more abundant in the motor cortex (M1/M2), as well as in the remaining subregions of the frontal cortex (i.e., dorsolateral orbital [DLO], lateral orbital [LO], and ventral orbital [VO] cortices). A high number of WFA+ PNNs was a common feature in the parietal cortex. In the primary somatosensory barrel field (S1BF), the number of WFA+ PNNs was higher than in the remaining subregions of the parietal cortex. The number of WFA+ PNNs was higher in the primary (V1 monocular [V1 M] and V1 binocular [V1B]), relative to the secondary (V2 mediomedial [V2 M], V2 medial lateral [V2ML], and V2 lateral [V2L]) visual cortices of the occipital cortex. WFA+ PNNs were highly abundant in all subregions of the auditory cortex (i.e., primary auditory [Au1], as well as secondary auditory, dorsal [AuD], and ventral [AuV] areas). The number of WFA+ PNNs in subregions of the entorhinal cortex (perirhinal [PRh], dorsolateral entorhinal [DLEnt], and dorsolateral entorhinal [DLEnt]) was significantly lower when compared to that in the auditory cortices. The number of WFA+ PNNs in the retrosplenial cortex was significantly higher than in the other cortices .

Further, we quantified AB1031-positive (AB1031+) PNNs in the mouse cerebral cortex (Fig. 5**B**). The density of AB1031+ PNNs showed significantly different variations throughout the mouse cortical regions examined. In many regions (i.e., frontal association [FrA], Cg, PL, IL, DP, temporal association [TeA], ectorhinal [Ect], PRh, DLEnt, and DIEnt), AB1031+ PNNs were very low compared with other cortices. In the frontal cortex, a high number of AB1031+ PNNs was observed in the DLO, LO, and VO subregions. In the remaining subregions of the frontal cortex (primary and secondary motor areas [M1 and M2, respectively]), the density of AB1031+ PNNs was high compared to that in the frontal cortex subregions, FrA, Cg, PL, IL, and DP. In the S1BF subregion, the number of AB1031+ PNNs was higher than in the remaining subregions of the parietal cortex (i.e., medial parietal association [MPtA], lateral parietal association [LPtA], somatosensory 1, trunk region [S1Tr], and somatosensory 2 [S2] areas). In the temporal cortex, subregions of the auditory cortex (i.e., AuV, Au1, and AuD) exhibited high AB1031+ PNN densities, followed by lower densities in the entorhinal cortex subregions (i.e., TeA, Ect, PRh, DIEnt, and DLEnt). Finally, the number of AB1031+ PNNs in subregions of the retrosplenial cortex was significantly higher than in other cortices.

3.3. Co-localization of WFA+ and AB1031+ PNNs

Further, we determined the percentage of overlapping WFA+ and AB1031+ PNNs in the mouse cerebral cortex (Fig. 5**C**), and determined this value to be below 50% in many regions. More specifically, the percentage of co-localized WFA+ and AB1031+ PNNs in the FrA, Cg, PL, IL, and DP subregions of the frontal cortex was lower than in the remaining subregions (i.e., DLO, LO, VO, M1, and M2). Approximately 10% of WFA+ PNNs in the FrA, Cg, PL, IL, and

Table 1
P values for Figs. 5–6.

A: Fig. 5A — WFA+ PNNs / mm²

Frontal Cortex								**Parietal Cortex**				**Temporal Cortex**			
FrA	vs	DLO	0.0025	VO	vs	Cg	<0.0001	MPtA	vs	LPtA	0.1807	AuV	vs	Au1	0.0198
FrA	vs	LO	<0.0001	VO	vs	PL	<0.0001	MPtA	vs	S1Tr	0.0348	AuV	vs	AuD	0.9101
FrA	vs	VO	<0.0001	VO	vs	IL	<0.0001	MPtA	vs	S1BF	<0.0001	AuV	vs	TeA	0.0024
FrA	vs	Cg	0.2428	VO	vs	DP	<0.0001	MPtA	vs	S2	0.0305	AuV	vs	Ect	0.0002
FrA	vs	PL	0.0443	VO	vs	M1	<0.0001	LPtA	vs	S1Tr	0.3082	AuV	vs	PRh	<0.0001
FrA	vs	IL	0.1999	VO	vs	M2	<0.0001	LPtA	vs	S1BF	<0.0001	AuV	vs	DLEnt	<0.0001
FrA	vs	DP	0.0289	Cg	vs	PL	0.2048	LPtA	vs	S2	0.4426	AuV	vs	DIEnt	<0.0001
FrA	vs	M1	0.0229	Cg	vs	IL	0.8325	S1Tr	vs	S1BF	0.0041	Au1	vs	AuD	0.0148
FrA	vs	M2	0.7034	Cg	vs	DP	0.1261	S1Tr	vs	S2	0.6562	Au1	vs	TeA	<0.0001
DLO	vs	LO	0.0002	Cg	vs	M1	<0.0001	S1BF	vs	S2	<0.0001	Au1	vs	Ect	<0.0001
DLO	vs	VO	0.0003	Cg	vs	M2	0.0246	**Occipital Cortex**				Au1	vs	PRh	<0.0001
DLO	vs	Cg	0.0053	PL	vs	IL	0.3234	V2MM	vs	V2ML	0.041	Au1	vs	DLEnt	<0.0001
DLO	vs	PL	<0.0001	PL	vs	DP	0.7341	V2MM	vs	V1M	<0.0001	Au1	vs	DIEnt	<0.0001
DLO	vs	IL	<0.0001	PL	vs	M1	<0.0001	V2MM	vs	V1B	<0.0001	AuD	vs	TeA	0.0033
DLO	vs	DP	<0.0001	PL	vs	M2	0.0006	V2MM	vs	V2L	0.0035	AuD	vs	Ect	0.0003
DLO	vs	M1	0.1901	IL	vs	DP	0.2093	V2ML	vs	V1M	<0.0001	AuD	vs	PRh	<0.0001
DLO	vs	M2	0.0003	IL	vs	M1	<0.0001	V2ML	vs	V1B	<0.0001	AuD	vs	DLEnt	<0.0001
LO	vs	VO	0.7967	IL	vs	M2	0.0201	V2ML	vs	V2L	0.3587	AuD	vs	DIEnt	<0.0001
LO	vs	Cg	<0.0001	DP	vs	M1	<0.0001	V1M	vs	V1B	0.6917	TeA	vs	Ect	0.4414
LO	vs	PL	<0.0001	DP	vs	M2	0.0004	V1M	vs	V2L	0.0001	TeA	vs	PRh	<0.0001
LO	vs	IL	<0.0001	M1	vs	M2	0.0055	V1B	vs	V2L	<0.0001	TeA	vs	DLEnt	<0.0001
LO	vs	DP	<0.0001					**Retrosplenial Cortex**				TeA	vs	DIEnt	<0.0001
LO	vs	M1	<0.0001					RSD	vs	RSGa	0.0464	Ect	vs	PRh	0.0001
LO	vs	M2	<0.0001					RSD	vs	RSGb	0.544	Ect	vs	DLEnt	<0.0001
								RSD	vs	RSGc	0.5042	Ect	vs	DIEnt	<0.0001
								RSGa	vs	RSGb	0.1759	PRh	vs	DLEnt	0.7486
								RSGa	vs	RSGc	0.1609	PRh	vs	DIEnt	0.1735
								RSGb	vs	RSGc	0.9814	DLEnt	vs	DIEnt	0.2959

B: Fig. 5B — AB1031+ PNNs / mm²

Frontal Cortex								**Parietal Cortex**				**Temporal Cortex**			
FrA	vs	DLO	<0.0001	VO	vs	Cg	<0.0001	MPtA	vs	LPtA	0.012	AuV	vs	Au1	<0.0001
FrA	vs	LO	<0.0001	VO	vs	PL	<0.0001	MPtA	vs	S1Tr	<0.0001	AuV	vs	AuD	0.3619
FrA	vs	VO	<0.0001	VO	vs	IL	<0.0001	MPtA	vs	S1BF	<0.0001	AuV	vs	TeA	<0.0001
FrA	vs	Cg	0.6815	VO	vs	DP	<0.0001	MPtA	vs	S2	<0.0001	AuV	vs	Ect	0.0003
FrA	vs	PL	0,4445	VO	vs	M1	<0.0001	LPtA	vs	S1Tr	0.0017	AuV	vs	PRh	<0.0001
FrA	vs	IL	0.3161	VO	vs	M2	<0.0001	LPtA	vs	S1BF	<0.0001	AuV	vs	DLEnt	<0.0001
FrA	vs	DP	0.3697	Cg	vs	PL	0.664	LPtA	vs	S2	0.016	AuV	vs	DIEnt	<0.0001
FrA	vs	M1	<0.0001	Cg	vs	IL	0.4662	S1Tr	vs	S1BF	<0.0001	Au1	vs	AuD	<0.0001
FrA	vs	M2	0.0399	Cg	vs	DP	0,5484	S1Tr	vs	S2	0.2349	Au1	vs	TeA	<0.0001
DLO	vs	LO	0.0084	Cg	vs	M1	<0.0001	S1BF	vs	S2	<0.0001	Au1	vs	Ect	<0.0001
DLO	vs	VO	0.0002	Cg	vs	M2	0.0026	**Occipital Cortex**				Au1	vs	PRh	<0.0001
DLO	vs	Cg	<0.0001	PL	vs	IL	0.7602	V2MM	vs	V2ML	0.1345	Au1	vs	DLEnt	<0.0001
DLO	vs	PL	<0.0001	PL	vs	DP	0.8599	V2MM	vs	V1M	<0.0001	Au1	vs	DIEnt	<0.0001
DLO	vs	IL	<0.0001	PL	vs	M1	<0.0001	V2MM	vs	V1B	<0.0001	AuD	vs	TeA	<0.0001
DLO	vs	DP	<0.0001	PL	vs	M2	0.0006	V2MM	vs	V2L	0.0599	AuD	vs	Ect	0.0069
DLO	vs	M1	0.2827	IL	vs	DP	0.8999	V2ML	vs	V1M	<0.0001	AuD	vs	PRh	<0.0001
DLO	vs	M2	0.0003	IL	vs	M1	<0.0001	V2ML	vs	V1B	<0.0001	AuD	vs	DLEnt	<0.0001
LO	vs	VO	0.1678	IL	vs	M2	0.0002	V2ML	vs	V2L	0.7072	AuD	vs	DIEnt	<0.0001
LO	vs	Cg	<0.0001	DP	vs	M1	<0.0001	V1M	vs	V1B	0.4069	TeA	vs	Ect	0.0007
LO	vs	PL	<0.0001	DP	vs	M2	0.0004	V1M	vs	V2L	<0.0001	TeA	vs	PRh	0.8235
LO	vs	IL	<0.0001	M1	vs	M2	0.0011	V1B	vs	V2L	<0.0001	TeA	vs	DLEnt	0.843
LO	vs	DP	<0.0001					**Retrosplenial Cortex**				TeA	vs	DIEnt	0.5046
LO	vs	M1	<0.0001					RSD	vs	RSGa	<0.0001	Ect	vs	PRh	0.0003
LO	vs	M2	<0.0001					RSD	vs	RSGb	0.0001	Ect	vs	DLEnt	0.0003
								RSD	vs	RSGc	0.2784	Ect	vs	DIEnt	0.0005
								RSGa	vs	RSGb	0.0004	PRh	vs	DLEnt	0.9797
								RSGa	vs	RSGc	<0.0001	PRh	vs	DIEnt	0.6527
								RSGb	vs	RSGc	0.0698	DLEnt	vs	DIEnt	0.6345

Table 1 (*Continued*)

C: Fig. 5C — AB1031+ PNNs / WFA+ PNNs (%)

Frontal Cortex							
FrA	vs	DLO	0.0017	VO	vs	Cg	0.0003
FrA	vs	LO	0.003	VO	vs	PL	<0.0001
FrA	vs	VO	0.0038	VO	vs	IL	<0.0001
FrA	vs	Cg	0.7328	VO	vs	DP	0.0036
FrA	vs	PL	0.8156	VO	vs	M1	0.7913
FrA	vs	IL	0.7461	VO	vs	M2	0.3727
FrA	vs	DP	0.4426	Cg	vs	PL	0.3987
FrA	vs	M1	0.0016	Cg	vs	IL	0.3506
FrA	vs	M2	0.0176	Cg	vs	DP	0.5331
DLO	vs	LO	0.6843	Cg	vs	M1	<0.0001
DLO	vs	VO	0.6171	Cg	vs	M2	0.0029
DLO	vs	Cg	0.0001	PL	vs	IL	0.8896
DLO	vs	PL	<0.0001	PL	vs	DP	0.1581
DLO	vs	IL	<0.0001	PL	vs	M1	<0.0001
DLO	vs	DP	0.0015	PL	vs	M2	0.0002
DLO	vs	M1	0.7794	IL	vs	DP	0.1418
DLO	vs	M2	0.1815	IL	vs	M1	<0.0001
LO	vs	VO	0.9194	IL	vs	M2	0.0003
LO	vs	Cg	0.0002	DP	vs	M1	0.0009
LO	vs	PL	0.0001	DP	vs	M2	0.0261
LO	vs	IL	<0.0001	M1	vs	M2	0.2216
LO	vs	DP	0.0027				
LO	vs	M1	0.8744				
LO	vs	M2	0.3188				

Parietal Cortex							
MPtA	vs	LPtA	0.3152				
MPtA	vs	S1Tr	0.0888				
MPtA	vs	S1BF	0.0003				
MPtA	vs	S2	0.0039				
LPtA	vs	S1Tr	0.3834				
LPtA	vs	S1BF	0.0062				
LPtA	vs	S2	0.054				
S1Tr	vs	S1BF	0.143				
S1Tr	vs	S2	0.4715				
S1BF	vs	S2	0.3152				
Occipital Cortex							
V2MM	vs	V2ML	0.1993				
V2MM	vs	V1M	0.0025				
V2MM	vs	V1B	0.0008				
V2MM	vs	V2L	0.1182				
V2ML	vs	V1M	0.0695				
V2ML	vs	V1B	0.0307				
V2ML	vs	V2L	0.7985				
V1M	vs	V1B	0.7043				
V1M	vs	V2L	0.1064				
V1B	vs	V2L	0.0484				
Retrosplenial Cortex							
RSD	vs	RSGa	0.4697				
RSD	vs	RSGb	0.427				
RSD	vs	RSGc	0.2265				
RSGa	vs	RSGb	0.0104				
RSGa	vs	RSGc	0.0028				
RSGb	vs	RSGc	0.7226				

Temporal Cortex							
AuV	vs	Au1	0.2105				
AuV	vs	AuD	0.3723				
AuV	vs	TeA	0.0016				
AuV	vs	Ect	0.7153				
AuV	vs	PRh	0.0053				
AuV	vs	DLEnt	0.0017				
AuV	vs	DIEnt	0.0017				
Au1	vs	AuD	0.0341				
Au1	vs	TeA	0.0002				
Au1	vs	Ect	0.1076				
Au1	vs	PRh	<0.0001				
Au1	vs	DLEnt	0.0003				
Au1	vs	DIEnt	0.0003				
AuD	vs	TeA	0.0197				
AuD	vs	Ect	0.5966				
AuD	vs	PRh	0.0518				
AuD	vs	DLEnt	0.0182				
AuD	vs	DIEnt	0.0182				
TeA	vs	Ect	0.0047				
TeA	vs	PRh	0.6847				
TeA	vs	DLEnt	0.8661				
TeA	vs	DIEnt	0.8661				
Ect	vs	PRh	0.0144				
Ect	vs	DLEnt	0.0047				
Ect	vs	DIEnt	0.0047				
PRh	vs	DLEnt	0.5817				
PRh	vs	DIEnt	0.5817				
DLEnt	vs	DIEnt	1				

D: Fig. 5D — WFA+ PNNs / AB1031+ PNNs (%)

Frontal Cortex							
FrA	vs	DLO	0.7176	VO	vs	Cg	0.7809
FrA	vs	LO	0.4442	VO	vs	PL	0.8357
FrA	vs	VO	0.8357	VO	vs	IL	<0.0001
FrA	vs	Cg	1	VO	vs	DP	0.8357
FrA	vs	PL	1	VO	vs	M1	0.4318
FrA	vs	IL	<0.0001	VO	vs	M2	0.1929
FrA	vs	DP	1	Cg	vs	PL	1
FrA	vs	M1	0.5717	Cg	vs	IL	<0.0001
FrA	vs	M2	0.4226	Cg	vs	DP	1
DLO	vs	LO	0.4344	Cg	vs	M1	0.4447
DLO	vs	VO	0.7516	Cg	vs	M2	0.2793
DLO	vs	Cg	0.6325	PL	vs	IL	<0.0001
DLO	vs	PL	0.7176	PL	vs	DP	1
DLO	vs	IL	<0.0001	PL	vs	M1	0.5717
DLO	vs	DP	0.7176	PL	vs	M2	0.4226
DLO	vs	M1	0.6941	IL	vs	DP	<0.0001
DLO	vs	M2	0.3822	IL	vs	M1	<0.0001
LO	vs	VO	0.2385	IL	vs	M2	<0.0001
LO	vs	Cg	0.3061	DP	vs	M1	0.5717
LO	vs	PL	0.4441	DP	vs	M2	0.4226
LO	vs	IL	<0.0001	M1	vs	M2	0.5765
LO	vs	DP	0.4442				
LO	vs	M1	0.6425				
LO	vs	M2	0.95				

Parietal Cortex							
MPtA	vs	LPtA	0.7934				
MPtA	vs	S1Tr	0.1987				
MPtA	vs	S1BF	0.6527				
MPtA	vs	S2	0.6667				
LPtA	vs	S1Tr	0.1339				
LPtA	vs	S1BF	0.4643				
LPtA	vs	S2	0.4762				
S1Tr	vs	S1BF	0.3192				
S1Tr	vs	S2	0.3116				
S1BF	vs	S2	0.9827				
Occipital Cortex							
V2MM	vs	V2ML	0.0055				
V2MM	vs	V1M	0.0084				
V2MM	vs	V1B	0.0002				
V2MM	vs	V2L	0.0018				
V2ML	vs	V1M	0.6119				
V2ML	vs	V1B	0.3963				
V2ML	vs	V2L	0.7534				
V1M	vs	V1B	0.1226				
V1M	vs	V2L	0.3776				
V1B	vs	V2L	0.5909				
Retrosplenial Cortex							
RSD	vs	RSGa	0.0005				
RSD	vs	RSGb	0.0164				
RSD	vs	RSGc	0.6531				
RSGa	vs	RSGb	0.1813				
RSGa	vs	RSGc	0.0015				
RSGb	vs	RSGc	0.0432				

Temporal Cortex							
AuV	vs	Au1	0.743				
AuV	vs	AuD	0.8496				
AuV	vs	TeA	0.8577				
AuV	vs	Ect	0.2151				
AuV	vs	PRh	0.3513				
AuV	vs	DLEnt	0.0198				
AuV	vs	DIEnt	0.5572				
Au1	vs	AuD	0.8968				
Au1	vs	TeA	0.9452				
Au1	vs	Ect	0.3427				
Au1	vs	PRh	0.4764				
Au1	vs	DLEnt	0.0107				
Au1	vs	DIEnt	0.6543				
AuD	vs	TeA	0.9748				
AuD	vs	Ect	0.2965				
AuD	vs	PRh	0.4286				
AuD	vs	DLEnt	0.0152				
AuD	vs	DIEnt	0.6158				
TeA	vs	Ect	0.417				
TeA	vs	PRh	0.5048				
TeA	vs	DLEnt	0.0351				
TeA	vs	DIEnt	0.6481				
Ect	vs	PRh	1				
Ect	vs	DLEnt	0.0021				
Ect	vs	DIEnt	1				
PRh	vs	DLEnt	0.0103				
PRh	vs	DIEnt	1				
DLEnt	vs	DIEnt	0.0733				

Table 1 (*Continued*)

E: Fig. 6A — Cat-315+ PNNs / mm^2

Frontal Cortex							
FrA	vs	DLO	0.1879	VO	vs	Cg	<0.0001
FrA	vs	LO	0.0257	VO	vs	PL	<0.0001
FrA	vs	VO	<0.0001	VO	vs	IL	<0.0001
FrA	vs	Cg	0.6584	VO	vs	DP	<0.0001
FrA	vs	PL	0.2165	VO	vs	M1	0.0363
FrA	vs	IL	0.1719	VO	vs	M2	<0.0001
FrA	vs	DP	0.8083	Cg	vs	PL	0.0962
FrA	vs	M1	<0.0001	Cg	vs	IL	0.0733
FrA	vs	M2	0.0395	Cg	vs	DP	0.4943
DLO	vs	LO	0.7698	Cg	vs	M1	0.0001
DLO	vs	VO	0.0013	Cg	vs	M2	0.1009
DLO	vs	Cg	0.3122	PL	vs	IL	0.0733
DLO	vs	PL	0.0312	PL	vs	DP	0.3182
DLO	vs	IL	0.0249	PL	vs	M1	<0.0001
DLO	vs	DP	0.1381	PL	vs	M2	0.0015
DLO	vs	M1	0.0659	IL	vs	DP	0.2586
DLO	vs	M2	0.872	IL	vs	M1	<0.0001
LO	vs	VO	<0.0001	IL	vs	M2	0.001
LO	vs	Cg	0.0691	DP	vs	M1	<0.0001
LO	vs	PL	0.0008	DP	vs	M2	0.0224
LO	vs	IL	0.0006	M1	vs	M2	0.0188
LO	vs	DP	0.0142				
LO	vs	M1	0.0294				
LO	vs	M2	0.8523				
Parietal Cortex							
MPtA	vs	LPtA	0.4051				
MPtA	vs	S1Tr	0.0234				
MPtA	vs	S1BF	<0.0001				
MPtA	vs	S2	0.0161				
LPtA	vs	S1Tr	0.1331				
LPtA	vs	S1BF	<0.0001				
LPtA	vs	S2	0.1106				
S1Tr	vs	S1BF	0.0001				
S1Tr	vs	S2	0.9821				
S1BF	vs	S2	<0.0001				
Occipital Cortex							
V2MM	vs	V2ML	0.5425				
V2MM	vs	V1M	0.0005				
V2MM	vs	V1B	<0.0001				
V2MM	vs	V2L	0.0987				
V2ML	vs	V1M	0.0028				
V2ML	vs	V1B	< 0.0001				
V2ML	vs	V2L	0.2829				
V1M	vs	V1B	0.1062				
V1M	vs	V2L	0.0362				
V1B	vs	V2L	0.0006				
Retrosplenial Cortex							
RSD	vs	RSGa	0.0004				
RSD	vs	RSGb	0.5417				
RSD	vs	RSGc	0.0064				
RSGa	vs	RSGb	0.0029				
RSGa	vs	RSGc	<0.0001				
RSGb	vs	RSGc	0.0035				
Temporal Cortex							
AuV	vs	Au1	<0.0001				
AuV	vs	AuD	0.4884				
AuV	vs	TeA	0.0637				
AuV	vs	Ect	0.0018				
AuV	vs	PRh	0.0069				
AuV	vs	DLEnt	0.3664				
AuV	vs	DIEnt	0.0018				
Au1	vs	AuD	<0.0001				
Au1	vs	TeA	<0.0001				
Au1	vs	Ect	<0.0001				
Au1	vs	PRh	<0.0001				
Au1	vs	DLEnt	<0.0001				
Au1	vs	DIEnt	<0.0001				
AuD	vs	TeA	0.0141				
AuD	vs	Ect	0.0002				
AuD	vs	PRh	0.0011				
AuD	vs	DLEnt	0.0011				
AuD	vs	DIEnt	0.0002				
TeA	vs	Ect	0.173				
TeA	vs	PRh	0.3664				
TeA	vs	DLEnt	0.3711				
TeA	vs	DIEnt	0.173				
Ect	vs	PRh	0.6371				
Ect	vs	DLEnt	0.6307				
Ect	vs	DIEnt	1				
PRh	vs	DLEnt	0.9928				
PRh	vs	DIEnt	0.6371				
DLEnt	vs	DIEnt	0.6307				

F: Fig. 6B — Cat-316+ PNNs / mm^2

Frontal Cortex							
FrA	vs	DLO	0.0052	VO	vs	Cg	<0.0001
FrA	vs	LO	<0.0001	VO	vs	PL	<0.0001
FrA	vs	VO	<0.0001	VO	vs	IL	<0.0001
FrA	vs	Cg	0.7054	VO	vs	DP	<0.0001
FrA	vs	PL	0.6572	VO	vs	M1	<0.0001
FrA	vs	IL	1	VO	vs	M2	<0.0001
FrA	vs	DP	0.8637	Cg	vs	PL	0.9256
FrA	vs	M1	0.0016	Cg	vs	IL	0.5933
FrA	vs	M2	0.133	Cg	vs	DP	0.7702
DLO	vs	LO	0.0004	Cg	vs	M1	0.0001
DLO	vs	VO	0.0014	Cg	vs	M2	0.1108
DLO	vs	Cg	0.0024	PL	vs	IL	0.5308
DLO	vs	PL	0.0028	PL	vs	DP	0.7001
DLO	vs	IL	0.0008	PL	vs	M1	0.0002
DLO	vs	DP	0.0013	PL	vs	M2	0.1323
DLO	vs	M1	0.8093	IL	vs	DP	0.8083
DLO	vs	M2	0.0432	IL	vs	M1	<0.0001
LO	vs	VO	0.6008	IL	vs	M2	0.0361
LO	vs	Cg	<0.0001	DP	vs	M1	<0.0001
LO	vs	PL	<0.0001	DP	vs	M2	0.0614
LO	vs	IL	<0.0001	M1	vs	M2	0.0127
LO	vs	DP	<0.0001				
LO	vs	M1	<0.0001				
LO	vs	M2	<0.0001				
Parietal Cortex							
MPtA	vs	LPtA	0.1062				
MPtA	vs	S1Tr	0.0002				
MPtA	vs	S1BF	<0.0001				
MPtA	vs	S2	0.0018				
LPtA	vs	S1Tr	0.0067				
LPtA	vs	S1BF	<0.0001				
LPtA	vs	S2	0.0776				
S1Tr	vs	S1BF	0.0066				
S1Tr	vs	S2	0.1991				
S1BF	vs	S2	<0.0001				
Occipital Cortex							
V2MM	vs	V2ML	0.7465				
V2MM	vs	V1M	<0.0001				
V2MM	vs	V1B	<0.0001				
V2MM	vs	V2L	0.1201				
V2ML	vs	V1M	<0.0001				
V2ML	vs	V1B	<0.0001				
V2ML	vs	V2L	0.2114				
V1M	vs	V1B	0.8902				
V1M	vs	V2L	<0.0001				
V1B	vs	V2L	<0.0001				
Retrosplenial Cortex							
RSD	vs	RSGa	0.0668				
RSD	vs	RSGb	0.3277				
RSD	vs	RSGc	0.6879				
RSGa	vs	RSGb	0.0081				
RSGa	vs	RSGc	0.0294				
RSGb	vs	RSGc	0.558				
Temporal Cortex							
AuV	vs	Au1	0.0326				
AuV	vs	AuD	0.1075				
AuV	vs	TeA	<0.0001				
AuV	vs	Ect	0.0016				
AuV	vs	PRh	<0.0001				
AuV	vs	DLEnt	<0.0001				
AuV	vs	DIEnt	<0.0001				
Au1	vs	AuD	0.0004				
Au1	vs	TeA	<0.0001				
Au1	vs	Ect	<0.0001				
Au1	vs	PRh	<0.0001				
Au1	vs	DLEnt	<0.0001				
Au1	vs	DIEnt	<0.0001				
AuD	vs	TeA	0.0029				
AuD	vs	Ect	0.078				
AuD	vs	PRh	0.0029				
AuD	vs	DLEnt	0.0016				
AuD	vs	DIEnt	0.0026				
TeA	vs	Ect	0.1997				
TeA	vs	PRh	0.8873				
TeA	vs	DLEnt	0.9586				
TeA	vs	DIEnt	0.9131				
Ect	vs	PRh	0.2298				
Ect	vs	DLEnt	0.1651				
Ect	vs	DIEnt	0.2178				
PRh	vs	DLEnt	0.8392				
PRh	vs	DIEnt	0.9727				
DLEnt	vs	DIEnt	0.8659				

Table 1 (*Continued*)

G: Fig. 6C — Cat-315+ PNNs / AB1031+ PNNs (%)

Frontal Cortex								**Parietal Cortex**				**Temporal Cortex**			
FrA	vs	DLO	0.9812	VO	vs	Cg	0.9751	MPtA	vs	LPtA	0.9042	AuV	vs	Au1	0.0007
FrA	vs	LO	0.8194	VO	vs	PL	0.2426	MPtA	vs	S1Tr	0.6842	AuV	vs	AuD	0.0568
FrA	vs	VO	0.2297	VO	vs	IL	0.0509	MPtA	vs	S1BF	0.0871	AuV	vs	TeA	0.2413
FrA	vs	Cg	0.2951	VO	vs	DP	0.2426	MPtA	vs	S2	0.2953	AuV	vs	Ect	0.0729
FrA	vs	PL	0.0749	VO	vs	M1	0.168	LPtA	vs	S1Tr	0.5466	AuV	vs	PRh	0.2413
FrA	vs	IL	0.1776	VO	vs	M2	0.4038	LPtA	vs	S1BF	0.0379	AuV	vs	DLEnt	0.2413
FrA	vs	DP	0.0749	Cg	vs	PL	0.2513	LPtA	vs	S2	0.1785	AuV	vs	DlEnt	0.2413
FrA	vs	M1	0.0132	Cg	vs	IL	0.061	S1Tr	vs	S1BF	0.0993	Au1	vs	AuD	0.0414
FrA	vs	M2	0.0532	Cg	vs	DP	0.2513	S1Tr	vs	S2	0.4283	Au1	vs	TeA	0.0017
DLO	vs	LO	0.89	Cg	vs	M1	0.2051	S1BF	vs	S2	0.31	Au1	vs	Ect	<0.0001
DLO	vs	VO	0.4055	Cg	vs	M2	0.4331	**Occipital Cortex**				Au1	vs	PRh	0.0017
DLO	vs	Cg	0.4461	PL	vs	IL	0.0199	V2MM	vs	V2ML	0.4141	Au1	vs	DLEnt	0.0017
DLO	vs	PL	0.1173	PL	vs	DP	1	V2MM	vs	V1M	0.2244	Au1	vs	DlEnt	0.0017
DLO	vs	IL	0.2269	PL	vs	M1	0.6654	V2MM	vs	V1B	0.1046	AuD	vs	TeA	0.024
DLO	vs	DP	0.1173	PL	vs	M2	0.4845	V2MM	vs	V2L	0.1157	AuD	vs	Ect	0.0009
DLO	vs	M1	0.0755	IL	vs	DP	0.0199	V2ML	vs	V1M	0.666	AuD	vs	PRh	0.0241
DLO	vs	M2	0.1616	IL	vs	M1	0.0092	V2ML	vs	V1B	0.3777	AuD	vs	DLEnt	0.0241
LO	vs	VO	0.327	IL	vs	M2	0.0194	V2ML	vs	V2L	0.39	AuD	vs	DlEnt	0.024
LO	vs	Cg	0.3966	DP	vs	M1	0.6654	V1M	vs	V1B	0.6482	TeA	vs	Ect	1
LO	vs	PL	0.0952	DP	vs	M2	0.4845	V1M	vs	V2L	0.6501	TeA	vs	PRh	1
LO	vs	IL	0.1432	M1	vs	M2	0.6196	V1B	vs	V2L	0.9859	TeA	vs	DLEnt	1
LO	vs	DP	0.0952					**Retrosplenial Cortex**				TeA	vs	DlEnt	1
LO	vs	M1	0.0226					RSD	vs	RSGa	0.1749	Ect	vs	PRh	1
LO	vs	M2	0.0828					RSD	vs	RSGb	0.9902	Ect	vs	DLEnt	1
								RSD	vs	RSGc	0.2489	Ect	vs	DlEnt	1
								RSGa	vs	RSGb	0.217	PRh	vs	DLEnt	1
								RSGa	vs	RSGc	0.0268	PRh	vs	DlEnt	1
								RSGb	vs	RSGc	0.2908	DLEnt	vs	DlEnt	1

H: Fig. 6D — Cat-316+ PNNs / AB1031+ PNNs (%)

Frontal Cortex								**Parietal Cortex**				**Temporal Cortex**			
FrA	vs	DLO	0.0895	VO	vs	Cg	0.8069	MPtA	vs	LPtA	0.0605	AuV	vs	Au1	0.4166
FrA	vs	LO	0.0049	VO	vs	PL	0.7294	MPtA	vs	S1Tr	0.0202	AuV	vs	AuD	0.9726
FrA	vs	VO	0.006	VO	vs	IL	0.006	MPtA	vs	S1BF	0.0047	AuV	vs	TeA	0.4279
FrA	vs	Cg	0.0123	VO	vs	DP	0.5185	MPtA	vs	S2	0.0224	AuV	vs	Ect	0.5732
FrA	vs	PL	0.0213	VO	vs	M1	0.5917	LPtA	vs	S1Tr	0.4731	AuV	vs	PRh	0.0919
FrA	vs	IL	1	VO	vs	M2	0.0406	LPtA	vs	S1BF	0.2617	AuV	vs	DLEnt	0.1222
FrA	vs	DP	0.009	Cg	vs	PL	0.9031	LPtA	vs	S2	0.6397	AuV	vs	DlEnt	0.9931
FrA	vs	M1	0.011	Cg	vs	IL	0.0123	S1Tr	vs	S1BF	0.7671	Au1	vs	AuD	0.3976
FrA	vs	M2	0.0759	Cg	vs	DP	0.4443	S1Tr	vs	S2	0.7631	Au1	vs	TeA	0.1511
DLO	vs	LO	0.1512	Cg	vs	M1	0.8351	S1BF	vs	S2	0.5057	Au1	vs	Ect	0.1863
DLO	vs	VO	0.182	Cg	vs	M2	0.1223	**Occipital Cortex**				Au1	vs	PRh	0.0195
DLO	vs	Cg	0.2983	PL	vs	IL	0.0213	V2MM	vs	V2ML	0.0309	Au1	vs	DLEnt	0.0316
DLO	vs	PL	0.399	PL	vs	DP	0.4176	V2MM	vs	V1M	0.5469	Au1	vs	DlEnt	0.6565
DLO	vs	IL	0.0895	PL	vs	M1	0.9647	V2MM	vs	V1B	0.879	AuD	vs	TeA	0.4441
DLO	vs	DP	0.1406	PL	vs	M2	0.223	V2MM	vs	V2L	0.3267	AuD	vs	Ect	0.5955
DLO	vs	M1	0.3241	IL	vs	DP	0.009	V2ML	vs	V1M	0.0703	AuD	vs	PRh	0.0974
DLO	vs	M2	0.8428	IL	vs	M1	0.011	V2ML	vs	V1B	0.0258	AuD	vs	DLEnt	0.1286
LO	vs	VO	0.887	IL	vs	M2	0.0759	V2ML	vs	V2L	0.1518	AuD	vs	DlEnt	0.9921
LO	vs	Cg	0.7135	DP	vs	M1	0.3423	V1M	vs	V1B	0.6139	TeA	vs	Ect	0.7614
LO	vs	PL	0.6307	DP	vs	M2	0.0727	V1M	vs	V2L	0.6659	TeA	vs	PRh	0.4698
LO	vs	IL	0.0049	M1	vs	M2	0.1013	V1B	vs	V2L	0.3527	TeA	vs	DLEnt	0.4987
LO	vs	DP	0.5724					**Retrosplenial Cortex**				TeA	vs	DlEnt	0.6316
LO	vs	M1	0.4947					RSD	vs	RSGa	0.894	Ect	vs	PRh	0.2529
LO	vs	M2	0.0297					RSD	vs	RSGb	0.5058	Ect	vs	DLEnt	0.2927
								RSD	vs	RSGc	0.3893	Ect	vs	DlEnt	0.7614
								RSGa	vs	RSGb	0.5933	PRh	vs	DLEnt	1
								RSGa	vs	RSGc	0.4648	PRh	vs	DlEnt	0.3255
								RSGb	vs	RSGc	0.8415	DLEnt	vs	DlEnt	0.3408

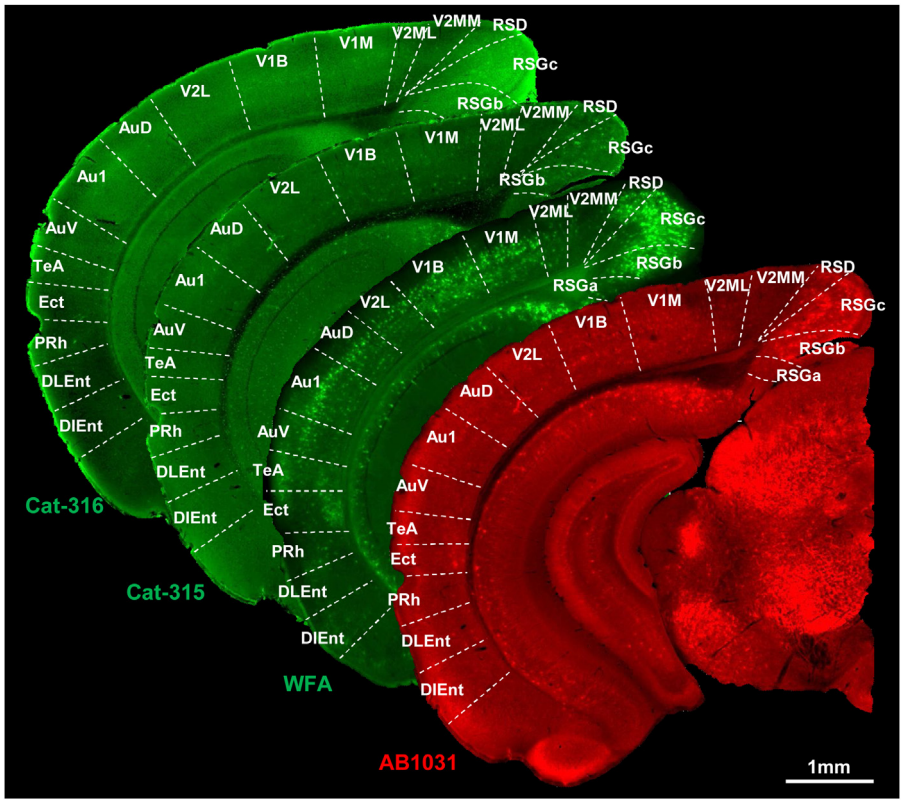

Fig. 3. Distribution of WFA-, AB1031-, Cat-315-, and Cat-316-positive PNNs in the mouse temporal cortex.
Representative whole brain sections labeled for WFA, AB1031, Cat-315, and Cat-316. Scale bar = 1 mm.

DP subregions of the frontal cortex were co-localized with AB1031. In the parietal cortex, the percentage of WFA+ PNNs co-localized with AB1031 was high, while WFA-AB1031 co-localization in MPtA/LPtA subregions of the parietal association cortex was low compared to the S1Tr/S1BF/S2 somatosensory cortex subregions. In the V1M/V1B subregions of the occipital cortex, the percentage of WFA-AB1031-positive PNNs was high compared to that in the V2MM/V2ML/V2L subregions of the secondary visual cortex. In the temporal cortex, the Au1/AuD/AuV subregions of the auditory cortex exhibited high percentages of WFA-AB1031 co-localization, followed by lower percentages in the TeA/PRh/DLEnt/DIEnt subregions of the entorhinal cortex. In all subregions of the retrosplenial cortex, about 40% of WFA+ PNNs co-localized with AB1031. Taken together, our findings revealed that AB1031-WFA co-localization was high (~80%) in the PNNs of most regions in the cerebral cortex (Fig. 5**D**). Note that IL/DP subregions of the frontal cortex were excluded from analysis since the number of AB1031+ PNNs was significantly low in these areas.

3.4. Comparative distribution of Cat-315- and Cat-316-positive PNNs

Further, we quantified the amount of PNNs co-labeled for Cat-315 and Cat-316 in the mouse cerebral cortex (Fig. 6**A,B**). The density of both Cat-315- and Cat-316-positive PNNs showed significantly different variations throughout the various cortical regions examined. In many areas (i.e., FrA, Cg, PL, IL, DP, TeA, Ect, PRh, DLEnt, and DIEnt), the number of both Cat-315- and Cat-316-positive PNNs was relatively low.

Cat-315 labeled many PNNs in the VO (Fig. 6**A**) and M1/M2 subregions of the motor cortex. In contrast, the density of Cat-315-positive PNNs was relatively low in the remaining subregions of the frontal cortex (i.e., FrA, Cg, PL, IL, and DP). In the parietal cortex, the Cat-315-positive PNN density was high, while in the MPtA/LPtA subregions of the parietal association cortex, Cat-315-positive PNN expression was low compared to the S1Tr/S1BF/S2 subregions of the somatosensory cortex. In the occipital cortex, low Cat-315-positive PNN density was observed in secondary (i.e., V2MM, V2ML, and V2L) compared to primary (i.e., V1M and V1B) subregions of the visual cortex. In the temporal cortex, Au1 exhibited high Cat-315-positive PNN density, followed by lower densities in AuV and AuD. The remaining subregions of the temporal cortex exhibited much lower Cat-315-positive PNNs than the other cortices. High numbers of Cat-315-positive PNNs were seen in the retrosplenial dysgranular cortex (RSD), as well as the b and c regions of the retrosplenial granular cortex (RSGb and RSGc, respectively). Cat-315-positive PNN density was lower in the remaining subregion of the retrosplenial cortex (i.e., RSGa).

In the LO/VO subregions of the frontal cortex, the density of Cat-316-positive PNNs was high compared to that in the remaining subregions (Fig. 6**B**). The FrA, Cg, PL, IL, and DP subregions exhibited lower Cat-316-positive PNN density relative to the DLO, LO, VO, M1, and M2 subregions of the frontal cortex. In the parietal cortex, low Cat-316-positive PNN density was observed in the MPtA/LPtA subregions of the association cortex. In the S1Tr, S1BF, and S2 subregions of the somatosensory cortex, the density of Cat-316-positive PNNs was high relative to that observed in the MPtA/LPtA subregions. In the occipital cortex, the density of Cat-316-positive PNNs in the primary visual cortex (i.e., V1M and V1B) was high compared to that observed in the secondary visual cortex (i.e., V2MM, V2ML, and V2L). In the temporal cortex, the Au1/AuD/AuV subregions of the auditory cortex exhibited high Cat-316-positive PNN densities, followed by lower densities in the TeA/Ect/PRh/DLEnt/DIEnt subregions of the entorhinal cortex. High numbers of Cat-316-positive PNNs were also seen in the RSD, RSGb, and RSGc subregions, while

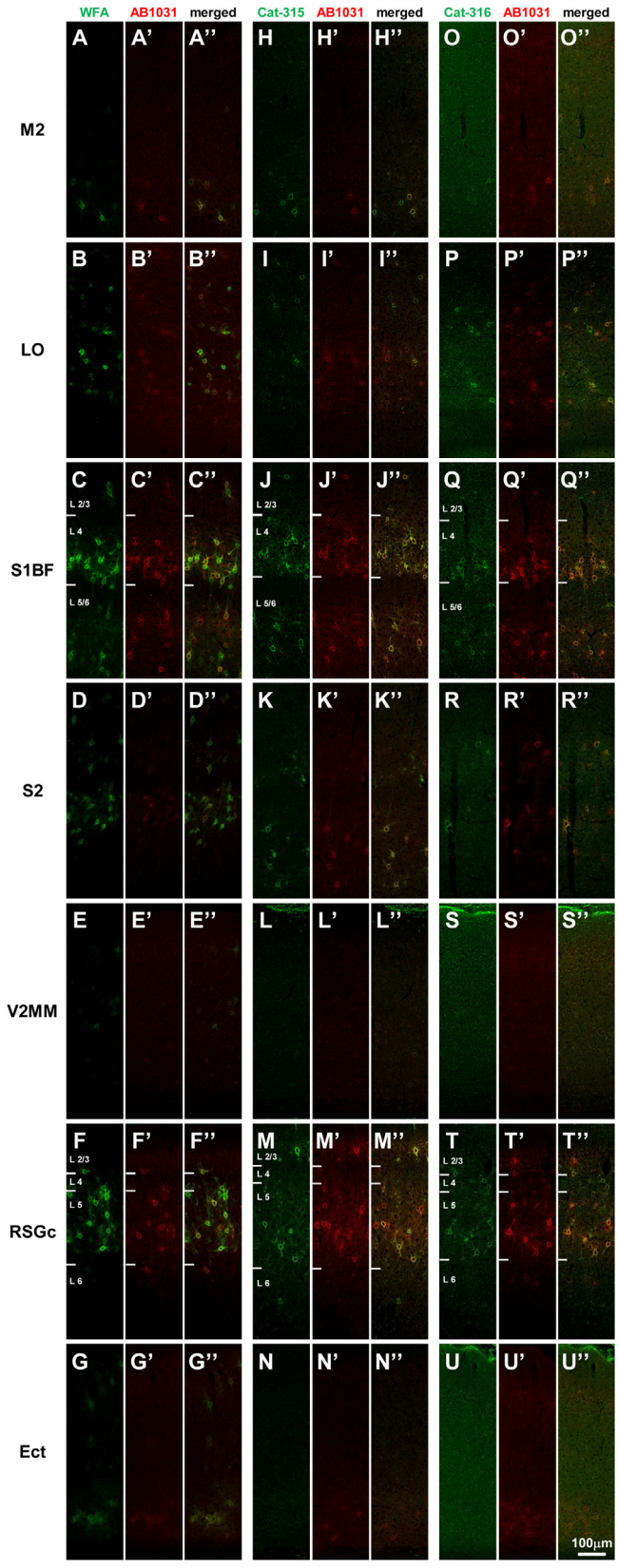

Fig. 4. Distribution patterns of WFA-, AB1031-, Cat-315-, and Cat-316-positive PNNs in the mouse cerebral cortex.
Confocal images of WFA (A-G) and AB1031 (A'-G') labeling, and the merged image (A"-G"). Confocal images of Cat-315 (H-N) and AB1031 (H'-N') labeling, and the merged image (H"-N"). Confocal images of Cat-316 (O-U) and AB1031 (O'-U') labeling, and the merged image (O"-U"). Images of M2 (A-A", H-H", O-O"), LO (B-B", I-I", P-P"), S1BF (C-C", J-J", Q-Q"), S2 (D-D", K-K", R-R"), V2MM (E-E", L-L", S-S"), RSGc (F-F", M-M", T-T"), and Ect (G-G", N-N", U-U"). Scale bar = 100 μm in U" (applies to A–U").

the remaining subregion of the retrosplenial cortex (i.e., RSGa) exhibited fewer Cat-316-positive PNNs.

3.5. Co-localization of Cat-315, Cat-316, and AB1031

In order to examine the relationship of aggrecan components in PNNs of the cerebral cortex, we carried out a quantitative analysis of AB1031 and Cat-315 co-localization, as well as of AB1031 and Cat-316 co-localization (Fig. 6**C and D**). Regions that exhibited low levels of AB1031 and Cat-315 labeling were excluded from the analysis (i.e., IL, DP, TeA, Ect, PRh, DLEnt, and DIEnt; Figs. 5**B** and 6**A,C**). In most other regions, AB1031+ PNNs also labeled with Cat-315 (Fig. 6**C**). This double-labeling was highest in all subregions of the parietal and retrosplenial cortices, and was also high in the PL subregion of the frontal cortex, as well as in the M1/M2 subregions of the motor cortex (~70%). In the remaining subregions of the frontal cortex (i.e., FrA, DLO, VO, and Cg), about half of the AB1031+ PNNs were positive for Cat-315. In the V2MM/V2ML subregions of the occipital cortex, a low percentage of AB1031+ PNNs co-localized with Cat-315. In the temporal cortex, Au1 exhibited a higher percentage of AB1031-Cat-315 co-localization relative to the remaining auditory cortex subregions (i.e., AuV and AuD).

Regarding the evaluation of PNNs double-labeled for AB1031 and Cat-316, regions which exhibited little individual labeling of AB1031 and Cat-316 (i.e., FrA and IL) were excluded from the analysis (Figs. 5**B** and 6**B**,**D**). In the frontal cortex, the percentage of AB1031+ PNNs that also labeled for Cat-316 was about 70%. In the MPtA subregion of the parietal cortex, about 50% of AB1031+ PNNs co-localized with Cat-316, while double labeling was higher (~70%) in the remaining subregions (i.e., LPtA, S1Tr, S1BF, and S2). The percentage of AB1031+ PNNs co-localized with Cat-316 in the V2ML subregion of the occipital cortex was lower than in the remaining subregions (i.e., V2MM, V1M, V1B, and V2L). The PRh/DLEnt subregions of the temporal cortex exhibited a lower number of AB1031+ PNNs co-localized with Cat-316 than the remaining subregions of the temporal cortex. Finally, the percentage of AB1031+ PNNs that also labeled with Cat-316 was similar throughout all subregions of the retrosplenial cortex.

3.6. Perisomatic distribution patterns of WFA-, AB1031-, Cat-315-, and Cat-316-positive PNN components

To address the perisomatic distribution of WFA-, AB1031-, Cat-315-, and Cat-316-positive PNN components in the mouse cerebral cortex, we conducted high-magnification image analyses of stained sections. Using this approach, we found labeled components displayed a punctate distribution pattern around the soma (Fig. 7). Further, we found that AB1031+ puncta appeared close to, but did not overlap with, WFA+ molecules (Fig. 7**A–G**). Puncta co-labeled for Cat-315 and Cat-316 were also observed in PNNs (Fig. 7**H–N, O–U**) and, interestingly, these overlapped with PNN components positive for AB1031 (Fig. 7**H"–N", O"–U"**).

3.7. WFA+ molecules in the upper level of layer 1 of the PRh, DLEnt, and DIEnt

Since we observed intense WFA and Cat-316 reactivity in layer 1 of PRh/DLEnt/DIEnt subregions in the temporal cortex (Fig. 3), we decided to further analyze the composition of the labeled PNN components in this area. Low magnification views of WFA, AB1031, Cat-315, and Cat-316 reactivity within layer 1 showed similar associations between positively labeled components (Fig. 8**A–C**). High magnification images revealed AB1031-, Cat-315-, and Cat-316-positive molecules scattered throughout the upper level of layer 1 (Fig. 8**D–F** and **D'–F'**), and that WFA+ molecules did not co-localize with AB1031+ molecules in this area (Fig. 8**D–D"**). More-

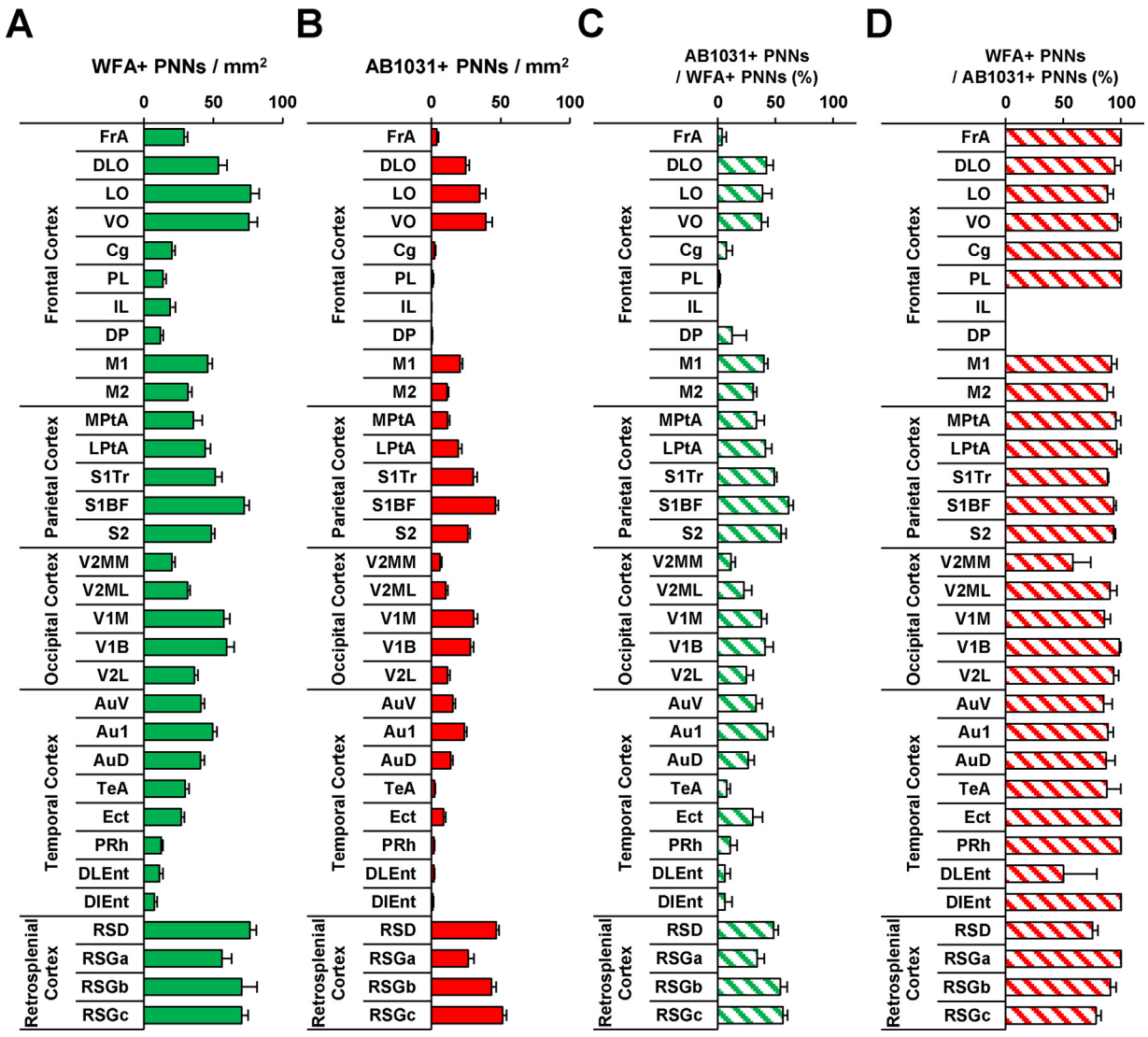

Fig. 5. Quantitative analyses of WFA- and AB1031-positive PNNs in the mouse cerebral cortex.
Quantified number of WFA+ PNNs in the mouse cerebral cortex (A). Quantified number of AB1031+ PNNs in the mouse cerebral cortex (B). The proportion of WFA+ PNNs co-localized with AB1031 (C), and the proportion of AB1031+ PNNs co-localized with WFA (D) in the mouse cerebral cortex. Data are expressed as the mean ± SEM. The respective *P* values are listed in Table 1.

over, AB1031+ molecules did not co-localize with either Cat-315+ or Cat-316+ molecules (Fig. 8**E–E"** and **F–F"**).

4. Discussion

This study was the first to quantitatively show region-specific distribution of PNNs in the mouse cortex through antibodies that recognize different aggrecan epitopes. Although WFA+ PNNs were present throughout the cortex, the existence of AB1031-, Cat-315-, and Cat-316-positive PNNs was disparate and region-specific. Together, our findings revealed 1) varied, brain region-specific aggrecan expression, 2) varied brain region-specific expression of aggrecan-positive PNN components, and 3) the existence of WFA+ PNNs without aggrecan in the mature mouse cortex.

Previous studies have reported the existence of region-selective WFA+ PNN expression throughout the mature rodent cortex (Brückner et al., 2000, 2003; Alpár et al., 2006; Horii-Hayashi et al., 2015). However, until now, WFA+ PNN densities in the various cortical regions had not been clarified. Our study revealed heterogeneous WFA+ PNN densities across the cortex, suggesting diverging, region-specific PNN functions.

A widely held theory is that WFA+ PNNs control plasticity. However, the expression of WFA+ PNNs has been observed throughout the cortex. As only certain cortical regions (e.g., the frontal cortex) are highly plastic over the course of an organism's lifetime (Sadato et al., 2004; Canto et al., 2008; Chapman et al., 2008; Jung et al., 2008; Kolb, 2009), it is unlikely that WFA+ PNN regulate plasticity in all cortices. Thus, WFA+ PNNs must have brain region-specific functions. Detection of PNNs using WFA is widely used but, as demonstrated in recent studies, PNN components are brain region- and cell type-specific (Berretta et al., 2015; Dauth et al., 2016; Ueno et al., 2017a). It is therefore plausible that the functions of WFA+ PNNs in each cortical region may differ depending on its components.

In the current study, we observed that almost all AB1031+ PNNs were also positive for WFA. However, in some regions of the mouse cortex, WFA+ PNNs could be detected in the absence of AB1031-, Cat-315-, and Cat-316-positive components. This is concurrent with previous findings, which have shown that aggrecan protein and aggrecan mRNA are not ubiquitously expressed in all cortical regions (Morawski et al., 2012a, 2012b). Several reports have suggested the possibility that aggrecan is involved in plasticity (McRae

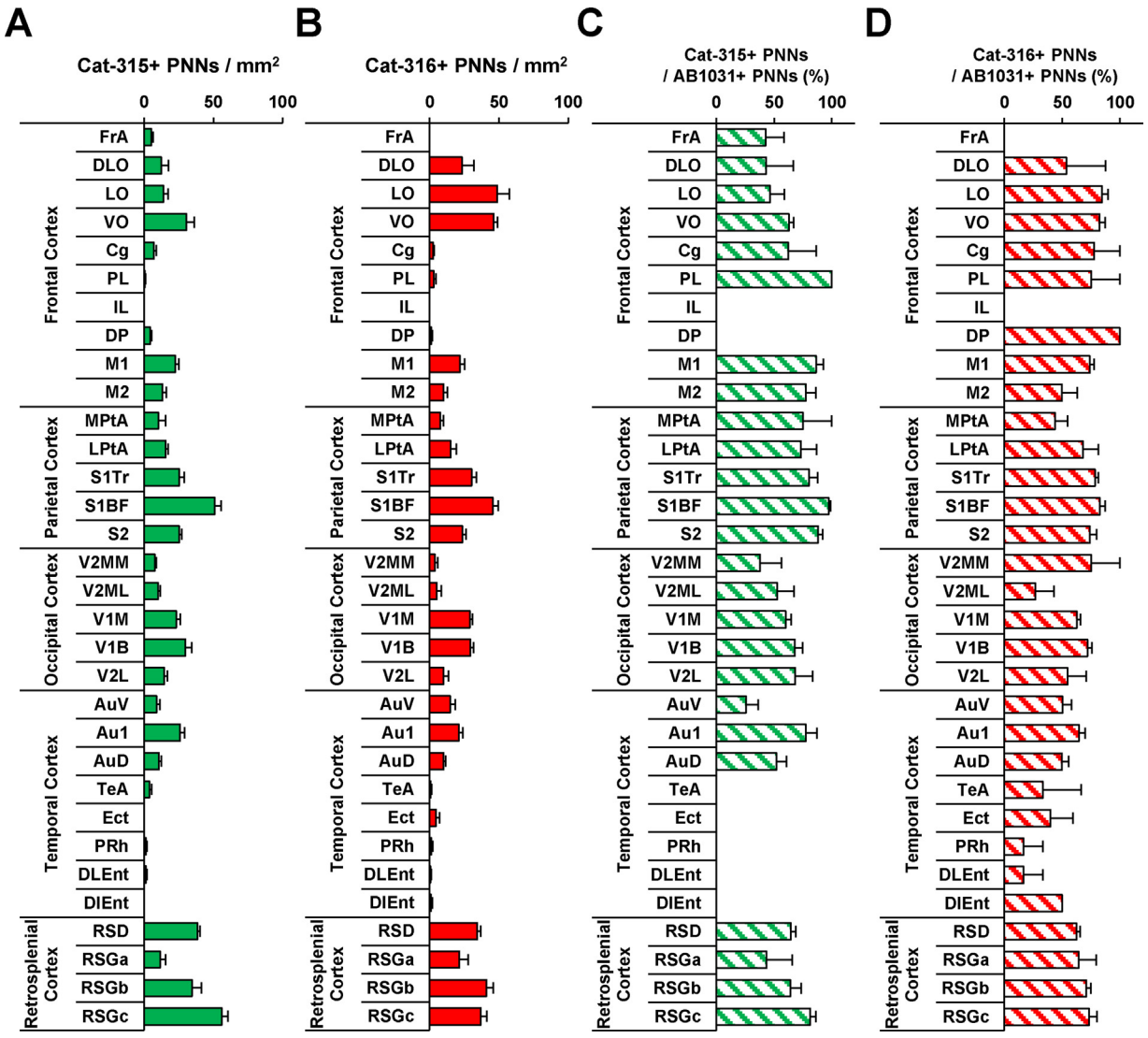

Fig. 6. Quantitative analyses of Cat-315- and Cat-316-positive PNNs in the mouse cerebral cortex.
Quantified number of Cat-315-positive PNNs in the mouse cerebral cortex (A). Quantified number of Cat-316-positive PNNs in the mouse cerebral cortex (B). The proportion of AB1031+ PNNs co-localized with Cat-315 (C), and the proportion of AB1031+ PNNs co-localized with Cat-316 (D) in the mouse cerebral cortex. Data are expressed as the mean ± SEM. The respective *P* values are listed in Table 1.

et al., 2007; Nakamura et al., 2009; Ye and Miao, 2013; Ueno et al., 2017b). Aggrecan expression in PNNs signals the end of the critical period, and is dependent on sensory input (Sur et al., 1988; Hockfield et al., 1990). In the absence of such input, the formation of both Cat-315- and Cat-316-positive, but not WFA+, PNNs decrease (McRae et al., 2007; Lander et al., 1997; Ueno et al., 2017a,b,c). This is because PNNs in the sensory cortex are formed during postnatal development, and AB1031- and Cat-315-positive PNNs are formed after WFA+ PNNs (Ueno et al., 2017a,b,c; Ye and Miao, 2013). In addition, WFA+ PNNs that do not have the Cat-315 epitope increase with age (Karetko-Sysa et al., 2014). Together, this suggests that neural plasticity is lost following the expression of aggrecan in WFA+ PNNs.

Previous reports have suggested that to access the backbone of the aggrecan molecule for staining with the AB1031 antibody, the sections must be treated with Chondroitinase ABC to remove the GAG chains (Härtig et al., 2016; Giamanco et al., 2010). Chondroitinase ABC treatment removes the GAG chain recognized by WFA. When this enzyme treatment is performed, double staining of WFA and AB1031 cannot be performed. However, it is also known that AB1031+ aggrecan can be sufficiently stained without this enzyme treatment (Carstens et al., 2016; Dauth et al., 2016; Miyata and Kitagawa, 2016; Yamada and Jinno, 2017). For these reasons, we performed double immunostaining without enzyme treatment in the present study. In order to compare the distributions of AB1031+ and WFA+ molecules in more detail, it is necessary to develop new experimental methods.

In recent years, it has been shown that the expression of a chondroitin sulfate group (recognized by Cat-316) in PNNs is involved in cortical plasticity (Matthews et al., 2002; Dino et al., 2006; Miyata et al., 2012). Moreover, the HNK-1 epitope (Dino et al., 2006) (recognized by Cat-315) has also been reported to relate to synaptic plasticity (Senn et al., 2002). Both chondroitin sulfate and HNK-1 are widely present in the central nervous system as ECM molecules (Kleene and Schachner, 2004). CSPGs and other ECM proteins inhibit plasticity and suppress the reformation of both axons and synapses (Gilbert et al., 2005; Silver and Silver, 2014). During CNS trauma, CSPG expression (including aggrecan) increases around the site of injury and suppresses axonal reorganization (Oohira et al., 1994; McKeon et al., 1999; Moon et al., 2002; Jones et al., 2003). *In vitro*, these functions are dependent on CSPG (versican, neurocan, brevican, and aggrecan) core proteins, which,

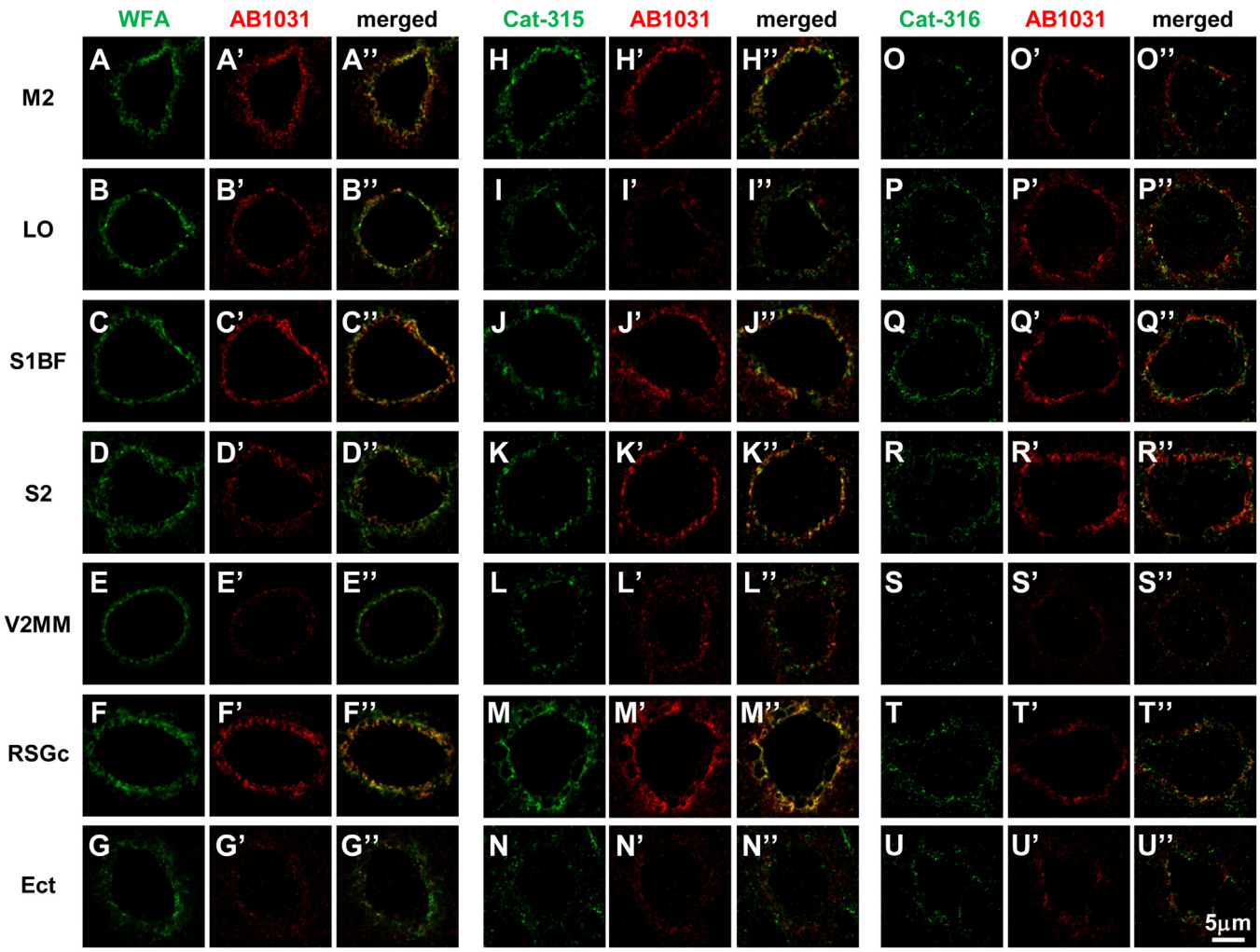

Fig. 7. Distribution patterns of WFA-, AB1031-, Cat-315-, and Cat-316-positive molecules in PNNs of the mouse cerebral cortex.
High-magnification confocal images of WFA (A-G) and AB1031 (A'-G') labeling, and the merged image (A"-G"). High-magnification confocal images of Cat-315 (H-N) and AB1031 (H'-N') labeling, and the merged image (H"-N"). High-magnification confocal images of Cat-316 (O-U) and AB1031 (O'-U') labeling, and the merged image (O"-U"). Images of M2 (A-A", H-H", O-O"), LO (B-B", I-I", P-P"), S1BF (C-C", J-J", Q-Q"), S2 (D-D", K-K", R-R"), V2MM (E-E", L-L", S-S"), RSGc (F-F", M-M", T-T"), and Ect (G-G", N-N", U-U") are shown. Scale bar = 5 μm in U" (applies to A–U").

after chondroitinase ABC treatment, have no inhibitory function (Snow et al., 1990; Maeda and Noda, 1996; Margolis et al., 1996; Yamada et al., 1997; Schmalfeldt et al., 2000). These reports indicate that the inhibitory functions of CSPGs and other ECM proteins are dependent on chondroitin sulfate chains rather than on CSPG core proteins. It is therefore possible that WFA+ PNNs that contain aggrecan expressing a chondroitin sulfate group control synaptic plasticity. Our findings suggest that plasticity may be high in areas where aggrecan expression is low. Indeed, we found that areas with low aggrecan corresponded to the prefrontal, entorhinal, and secondary sensory cortices, which have been shown to be highly plastic over the course of an organism's lifetime.

Compared to other lecticans, aggrecan is expressed on many PNNs (Matsui et al., 1998; Dauth et al., 2016), albeit in smaller amounts (Dauth et al., 2016). Generally, PNNs are thought to always contain aggrecan (Galtrey et al., 2008; Giamanco et al., 2010). Indeed, a previous study reported no WFA reactivity in primary cultured neurons of aggrecan-deficient mice, suggesting that aggrecan is essential for the formation of PNNs (Giamanco and Matthews, 2012). Conversely, some studies, including the current investigation, have reported the existence of WFA+ PNNs that do not contain aggrecan (Morawski et al., 2012a, 2012b; Karetko-Sysa et al., 2014; Ueno et al., 2017a), suggesting that aggrecan may not be an essential component in the PNNs of specific brain regions. Interestingly, it is indicated that absence of aggrecan has no effect on the expression patterns of other PNN markers, hyaluronan proteoglycan link protein 1, tenascin-R, hyaluronan, and brevican (Giamanco et al., 2010). It is reasonable to suggest that the constituent elements of PNN are brain-region specific.

It is difficult to clarify the distribution of the various PNN components using low magnification analysis. Therefore, until recent years, each component was considered to be consistent in its localization. Our previous study indicated divergent distributions of WFA- and Cat-315-positive molecules (Ueno et al., 2017b). High-magnification analysis in the current study corroborated these findings, revealing varied localization of WFA-, AB1031-, Cat-315-, and Cat-316-positive molecules. Even in the rat cortex, the distribution of aggrecan-positive PNNs is different depending on the antibody used to detect them (i.e., Cat-315 or AB1031) (Madinier et al., 2014). Lectin WFA and the monoclonal antibodies, AB1031, Cat-315, and Cat-316, recognize different aggrecan epitopes; thus, divergent distributions are reasonable. Moreover, it is possible that varied PNN component distributions are due to each CSPG being secreted from different cell types. For example, aggrecan seems to be secreted from PV-positive interneurons (Lander et al., 1998), while brevican has been shown to be secreted from neurons and

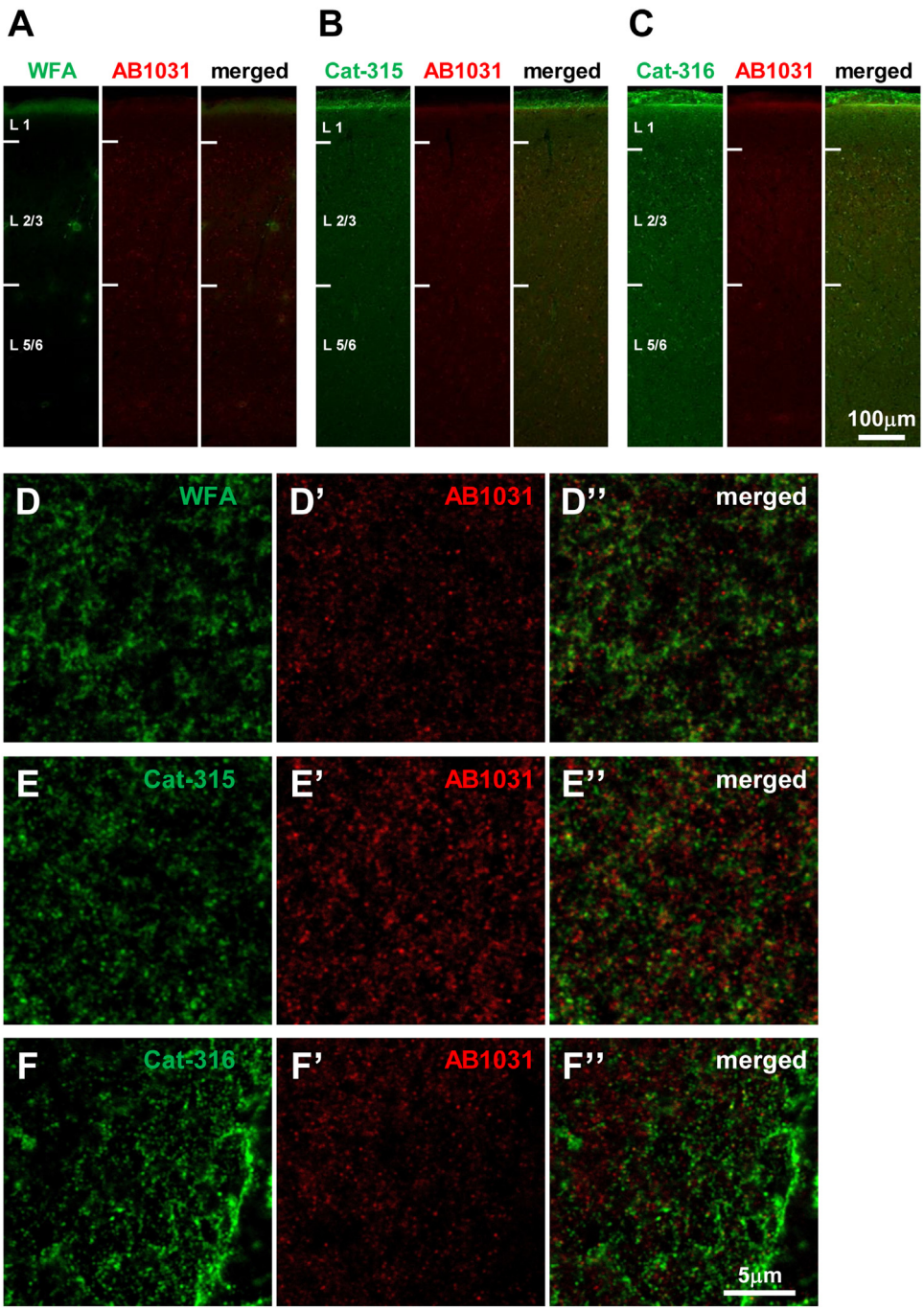

Fig. 8. Distribution of WFA-, AB1031-, Cat-315-, and Cat-316-positive molecules in the mouse entorhinal cortex.
Representative confocal images showing double labeling of WFA and AB1031 (A), Cat-315 and AB1031 (B), and Cat-316 and AB1031 (C) in the mouse entorhinal cortex. High magnification images of WFA (D') and AB1031 (D') labeling, and the merged image (D"), in the upper region of L1 in the DLEnt. High magnification images of Cat-315 (E) and AB1031 (E') labeling, and the merged image (E"), in the upper region of L1 in the DLEnt. High magnification images of Cat-316 (F) and AB1031 (F') labeling, and the merged image (F"), in the upper region of L1 in the DLEnt. Scale bar = 100 μm in C (applies to A–C) and 5 μm in F" (applies to D–F").

glia (Carulli et al., 2006). Regardless of the etiology for the distribution heterogeneity, these findings suggest that the various PNN components may have different functions, and that there is no single lectin or antibody that is capable of detecting all of the PNNs in the cortex.

While the detailed functions of PNNs remain unclear, ECM proteins are widely expressed in the central nervous system, particularly in the brainstem and cerebellum. Hence, it is assumed that these proteins must possess a protective function. Among the ECM family of proteins, aggrecan, tenascin-R, and the link proteins of PNNs are known to play neuroprotective roles (Morawski et al., 2012a, 2012b; Suttkus et al., 2014). Consistent with this, overexpression of aggrecan in the cortex is associated with less susceptibility to tau protein-induced cytotoxicity in Alzheimer's disease (Morawski et al., 2010). In addition, PNNs protect neurons from oxidative stress (Cabungcal et al., 2013; Ueno et al., 2017c), and PNN-rich brain regions are less susceptible to trauma (Harris et al., 2009). It has also been shown that PNNs and CSPGs are decreased in the entorhinal cortex of patients with schizophrenia (Pantazopoulos et al., 2010). Similarly, a decrease in prefrontal cor-

tex PNNs has also been observed in this patient population (Mauney et al., 2013). These reports indicate that CSPGs, such as PNNs, may be one of the underlying etiologies of schizophrenia, although it remains unclear why a decrease in PNNs does not appear in the sensory cortex of patients with schizophrenia. Interestingly, our current study revealed that aggrecan was either not present or expressed in very low levels in areas of the association cortex, where human studies have revealed decreased PNNs in patients with schizophrenia (i.e., the entorhinal and prefrontal subregions). Thus, PNNs in these brain areas may have little to no neuroprotective function.

It should be noted that there is some debate as to what WFA recognizes, as recent studies have questioned the assumption that the plant-derived lectin binds to the N-acetylgalactosamine of aggrecan (Karetko-Sysa et al., 2011; Miyata and Kitagawa, 2017; Ueno et al., 2017b). In our previous study, we found an accumulation of WFA+ molecules in the upper region of the temporal cortex. In previous studies, WFA-recognition molecules have been clearly shown, but no report has focused on them yet (Brückner et al., 2003; Horii-Hayashi et al., 2015; Yang et al., 2015). In the current study, AB1031-, Cat-315-, and Cat-316-positive molecules were observed to exist in this region, but they appeared uniform in each layer of the cortex. Layer 1 is special, as it contains no pyramidal cells. Instead, this layer comprises the axons of pyramidal cells in layers 2–6, as well as those of inhibitory interneurons and neurons from other cortical regions (Felleman and Van Essen, 1991; Vogt, 1991). Condensed WFA+ molecules are likely present because of some unknown role; thus, future studies should evaluate layer 1 of the temporal cortex, as it likely holds the key to clarifying which molecule is recognized by WFA, as well as its function.

5. Conclusions

The present clarified the region-specific expression of aggrecan components in the mature mouse cortex. Specifically showing divergent localizations of WFA-, AB1031-, Cat-315-, and Cat-316-positive PNN molecules. These results indicate that plasticity and neuroprotective function may differ depending on the cortical region, and provide useful insight for the development of methods to treat neuropsychiatric disorders and neurodegenerative diseases.

Author contributions

Study concept and design: H.U., M.O., and T.K. Data acquisition: H.U., K.F., K.T., and S.S. Data analysis and interpretation: H.U., K.F., K.T., and S.S. Drafting of the manuscript: H.U., M.O., and T.K. Critical revision of the manuscript for important intellectual content: S.M., N.K., K.W., S.A., and T.I. Statistical analyses: H.U and S.S. Study supervision: M.O. and T.I.

Funding sources

This research did not receive any specific grant from funding agencies in the public, commercial, or not-for-profit sectors.

Conflict of interest

The authors declare they have no competing financial interests.

Acknowledgements

We thank Kawasaki Medical School Central Research Institute for making instruments available to support this study. We thank Y. Koshidaka and M. Adachi for the technical assistance. The authors would also like to thank Editage (www.editage.jp) for English language editing.

References

Alpár, A., Gärtner, U., Härtig, W., Brückner, G., 2006. Distribution of pyramidal cells associated with perineuronal nets in the neocortex of rat. Brain Res. 1120, 13–22.
Balmer, T.S., Carels, V.M., Frisch, J.L., Nick, T.A., 2009. Modulation of perineuronal nets and parvalbumin with developmental song learning. J. Neurosci. 29, 12878–12885.
Bandtlow, C.E., Zimmermann, D.R., 2000. Proteoglycans in the developing brain: new conceptual insights for old proteins. Physiol. Rev. 80, 1267–1290.
Berretta, S., Pantazopoulos, H., Markota, M., Brown, C., Batzianouli, E.T., 2015. Losing the sugar coating: potential impact of perineuronal net abnormalities on interneurons in schizophrenia. Schizophr. Res. 167, 18–27.
Brückner, G., Brauer, K., Härtig, W., Wolff, J.R., Rickmann, M.J., Derouiche, A., Delpech, B., Girard, N., Oertel, W.H., Reichenbach, A., 1993. Perineuronal nets provide a polyanionic, glia-associated form of microenvironment around certain neurons in many parts of the rat brain. Glia 8, 183–200.
Brückner, G., Grosche, J., Schmidt, S., Härtig, W., Margolis, R.U., Delpech, B., Seidenbecher, C.I., Czaniera, R., Schachner, M., 2000. Postnatal development of perineuronal nets in wild-type mice and in a mutant deficient in tenascin-R. J. Comp. Neurol. 428, 616–629.
Brückner, G., Grosche, J., Hartlage-Rübsamen, M., Schmidt, S., Schachner, M., 2003. Region and lamina-specific distribution of extracellular matrix proteoglycans, hyaluronan and tenascin-R in the mouse hippocampal formation. J. Chem. Neuroanat. 26, 37–50.
Cabungcal, J.H., Steullet, P., Morishita, H., Kraftsik, R., Cuenod, M., Hensch, T.K., Do, K.Q., 2013. Perineuronal nets protect fast-spiking interneurons against oxidative stress. Proc. Natl. Acad. Sci. U. S. A. 110, 9130–9135.
Canto, C.B., Wouterlood, F.G., Witter, M.P., 2008. What does the anatomical organization of the entorhinal cortex tell us? Neural. Plast. 2008, 381243.
Carstens, K.E., Phillips, M.L., Pozzo-Miller, L., Weinberg, R.J., Dudek, S.M., 2016. Perineuronal nets suppress plasticity of excitatory synapses on CA2 pyramidal neurons. J. Neurosci. 36, 6312–6320.
Carulli, D., Rhodes, K.E., Brown, D.J., Bonnert, T.P., Pollack, S.J., Oliver, K., Strata, P., Fawcett, J.W., 2006. Composition of perineuronal nets in the adult rat cerebellum and the cellular origin of their components. J. Comp. Neurol. 494, 559–577.
Chapman, C.A., Jones, R.S., Jung, M., 2008. Neuronal plasticity in the entorhinal cortex. Neural. Plast. 2008, 314785.
Craig, S., Commins, S., 2006. The subiculum to entorhinal cortex projection is capable of sustaining both short- and long-term plastic changes. Behav. Brain Res. 174, 281–288.
Dauth, S., Grevesse, T., Pantazopoulos, H., Campbell, P.H., Maoz, B.M., Berretta, S., Parker, K.K., 2016. Extracellular matrix protein expression is brain region dependent. J. Comp. Neurol. 524, 1309–1336.
Dino, M.R., Harroch, S., Hockfield, S., Matthews, R.T., 2006. Monoclonal antibody Cat-315 detects a glycoform of receptor protein tyrosine phosphatase beta/phosphacan early in CNS development that localizes to extrasynaptic sites prior to synapse formation. Neuroscience 142, 1055–1069.
Felleman, D.J., Van Essen, D.C., 1991. Distributed hierarchical processing in the primate cerebral cortex. Cereb. Cortex 1, 1–47.
Foster, N.L., Mellott, J.G., Schofield, B.R., 2014. Perineuronal nets and GABAergic cells in the inferior colliculus of guinea pigs. Front. Neuroanat. 7, 53.
Galtrey, C.M., Kwok, J.C., Carulli, D., Rhodes, K.E., Fawcett, J.W., 2008. Distribution and synthesis of extracellular matrix proteoglycans hyaluronan, link proteins and tenascin-R in the rat spinal cord. Eur. J. Neurosci. 27, 1373–1390.
Gawryluk, J.W., Wang, J.F., Andreazza, A.C., Shao, L., Young, L.T., 2011. Decreased levels of glutathione, the major brain antioxidant, in post-mortem prefrontal cortex from patients with psychiatric disorders. Int. J. Neuropsychopharmacol. 14, 123–130.
Giamanco, K.A., Matthews, R.T., 2012. Deconstructing the perineuronal net: cellular contributions and molecular composition of the neuronal extracellular matrix. Neuroscience 218, 367–384.
Giamanco, K.A., Morawski, M., Matthews, R.T., 2010. Perineuronal net formation and structure in aggrecan knockout mice. Neuroscience 170, 1314–1327.
Gilbert, R.J., McKeon, R.J., Darr, A., Calabro, A., Hascall, V.C., Bellamkonda, R.V., 2005. CS-4,6 is differentially upregulated in glial scar and is a potent inhibitor of neurite extension. Mol. Cell Neurosci. 29, 545–558.
Gogolla, N., Caroni, P., Lüthi, A., Herry, C., 2009. Perineuronal nets protect fear memories from erasure. Science 325, 1258–1261.
Guimarães, A., Zaremba, S., Hockfield, S., 1990. Molecular and morphological changes in the cat lateral geniculate nucleus and visual cortex induced by visual deprivation are revealed by monoclonal antibodies Cat-304 and Cat-301. J. Neurosci. 10, 3014–3024.
Härtig, W., Brauer, K., Bigl, V., Brückner, G., 1994. Chondroitin sulfate proteoglycan-immunoreactivity of lectin-labeled perineuronal nets around parvalbumin-containing neurons. Brain Res. 635, 307–311.
Härtig, W., Appel, S., Suttkus, A., Grosche, J., Michalski, D., 2016. Abolished perineuronal nets and altered parvalbumin-immunoreactivity in the nucleus reticularis thalami of wildtype and 3xTg mice after experimental stroke. Neuroscience 337, 66–87.
Harris, N.G., Carmichael, S.T., Hovda, D.A., Sutton, R.L., 2009. Traumatic brain injury results in disparate regions of chondroitin sulfate proteoglycan expression that are temporally limited. J. Neurosci. Res. 87, 2937–2950.
Hensch, T.K., Fagiolini, M., 2005. Excitatory-inhibitory balance and critical period plasticity in developing visual cortex. Prog. Brain Res. 147, 115–124.

Hockfield, S., Kalb, R.G., Zaremba, S., Fryer, H., 1990. Expression of neural proteoglycans correlates with the acquisition of mature neuronal properties in the mammalian brain. Cold Spring Harb. Symp. Quant. Biol. 55, 505–514.
Horii-Hayashi, N., Sasagawa, T., Matsunaga, W., Nishi, M., 2015. Development and structural variety of the chondroitin sulfate proteoglycans-contained extracellular matrix in the mouse brain. Neural. Plast. 2015, 256389.
Jones, L.L., Sajed, D., Tuszynski, M.H., 2003. Axonal regeneration through regions of chondroitin sulfate proteoglycan deposition after spinal cord injury: a balance of permissiveness and inhibition. J. Neurosci. 23, 9276–9288.
Jung, M.W., Baeg, E.H., Kim, M.J., Kim, Y.B., Kim, J.J., 2008. Plasticity and memory in the prefrontal cortex. Rev. Neurosci. 19, 29–46.
Karetko-Sysa, M., Skangiel-Kramska, J., Nowicka, D., 2011. Disturbance of perineuronal nets in the perilesional area after photothrombosis is not associated with neuronal death. Exp. Neurol. 231, 113–126.
Karetko-Sysa, M., Skangiel-Kramska, J., Nowicka, D., 2014. Aging somatosensory cortex displays increased density of WFA-binding perineuronal nets associated with GAD-negative neurons. Neuroscience 277, 734–746.
Kleene, R., Schachner, M., 2004. Glycans and neural cell interactions. Nat. Rev. Neurosci. 5, 195–208.
Kolb, B., 2009. Brain and behavioural plasticity in the developing brain: neuroscience and public policy. Paediatr. Child Health 14, 651–652.
Lander, C., Kind, P., Maleski, M., Hockfield, S., 1997. A family of activity-dependent neuronal cell-surface chondroitin sulfate proteoglycans in cat visual cortex. J. Neurosci. 17, 1928–1939.
Lander, C., Zhang, H., Hockfield, S., 1998. Neurons produce a neuronal cell surface-associated chondroitin sulfate proteoglycan. J. Neurosci. 18, 174–183.
Lendvai, D., Morawski, M., Négyessy, L., Gáti, G., Jäger, C., Baksa, G., Glasz, T., Attems, J., Tanila, H., Arendt, T., Harkany, T., Alpár, A., 2013. Neurochemical mapping of the human hippocampus reveals perisynaptic matrix around functional synapses in Alzheimer's disease. Acta Neuropathol. 125, 215–229.
Madinier, A., Quattromani, M.J., Sjölund, C., Ruscher, K., Wieloch, T., 2014. Enriched housing enhances recovery of limb placement ability and reduces aggrecan-containing perineuronal nets in the rat somatosensory cortex after experimental stroke. PLoS One 9, e93121.
Maeda, N., Noda, M., 1996. 6B4 proteoglycan/phosphacan is a repulsive substratum but promotes morphological differentiation of cortical neurons. Development 122, 647–658.
Maffei, A., Turrigiano, G., 2008. The age of plasticity: developmental regulation of synaptic plasticity in neocortical microcircuits. Prog. Brain Res. 169, 211–223.
Margolis, R.K., Rauch, U., Maurel, P., Margolis, R.U., 1996. Neurocan and phosphacan: two major nervous tissue-specific chondroitin sulfate proteoglycans. Perspect. Dev. Neurobiol. 3, 273–290.
Matsui, F., Nishizuka, M., Yasuda, Y., Aono, S., Watanabe, E., Oohira, A., 1998. Occurrence of a N-terminal proteolytic fragment of neurocan, not a C-terminal half, in a perineuronal net in the adult rat cerebrum. Brain Res. 790, 45–51.
Matthews, R.T., Kelly, G.M., Zerillo, C.A., Gray, G., Tiemeyer, M., Hockfield, S., 2002. Aggrecan glycoforms contribute to the molecular heterogeneity of perineuronal nets. J. Neurosci. 22, 7536–7547.
Mauney, S.A., Athanas, K.M., Pantazopoulos, H., Shaskan, N., Passeri, E., Berretta, S., Woo, T.U.W., 2013. Developmental pattern of perineuronal nets in the human prefrontal cortex and their deficit in schizophrenia. Biol. Psychiatry 15, 427–435.
McKeon, R.J., Jurynec, M.J., Buck, C.R., 1999. The chondroitin sulfate proteoglycans neurocan and phosphacan are expressed by reactive astrocytes in the chronic CNS glial scar. J. Neurosci. 19, 10778–10788.
McRae, P.A., Rocco, M.M., Kelly, G., Brumberg, J.C., Matthews, R.T., 2007. Sensory deprivation alters aggrecan and perineuronal net expression in the mouse barrel cortex. J. Neurosci. 16, 5405–5413.
McRae, P.A., Baranov, E., Sarode, S., Brooks-Kayal, A.R., Porter, B.E., 2010. Aggrecan expression, a component of the inhibitory interneuron perineuronal net, is altered following an early-life seizure. Neurobiol. Dis. 39, 439–448.
Miyata, S., Kitagawa, H., 2016. Chondroitin 6-sulfation regulates perineuronal net formation by controlling the stability of aggrecan. Neural Plast., 1305801.
Miyata, S., Kitagawa, H., 2017. Formation and remodeling of the brain extracellular matrix in neural plasticity: roles of chondroitin sulfate and hyaluronan. Biochim. Biophys. Acta 1861, 2420–2434.
Miyata, S., Komatsu, Y., Yoshimura, Y., Taya, C., Kitagawa, H., 2012. Persistent cortical plasticity by upregulation of chondroitin 6-sulfation. Nat. Neurosci. 15, 414–422.
Moon, L.D.F., Asher, R.A., Rhodes, K.E., Fawcett, J.W., 2002. Relationship between sprouting axons, proteoglycans and glial cells following unilateral nigrostriatal axotomy in the adult rat. Neuroscience 109, 101–117.
Morawski, M., Brückner, G., Jäger, C., Seeger, G., Arendt, T., 2010. Neurons associated with aggrecan-based perineuronal nets are protected against tau pathology in subcortical regions in Alzheimer's disease. Neuroscience 169, 1347–1363.
Morawski, M., Brückner, G., Arendt, T., Matthews, R.T., 2012a. Aggrecan: beyond cartilage and into the brain. Int. J. Biochem. Cell Biol. 44, 690–693.
Morawski, M., Brückner, G., Jäger, C., Seeger, G., Matthews, R.T., Arendt, T., 2012b. Involvement of perineuronal and perisynaptic extracellular matrix in Alzheimer's disease neuropathology. Brain Pathol. 22, 547–561.
Morikawa, S., Ikegaya, Y., Narita, M., Tamura, H., 2017. Activation of perineuronal net-expressing excitatory neurons during associative memory encoding and retrieval. Sci. Rep. 7, 46024.
Nakamura, M., Nakano, K., Morita, S., Nakashima, T., Oohira, A., Miyata, S., 2009. Expression of chondroitin sulfate proteoglycans in barrel field of mouse and rat somatosensory cortex. Brain. Res. 1252, 117–129.
Oohira, A., Matsui, F., Watanabe, E., Kushima, Y., Maeda, N., 1994. Developmentally regulated expression of a brain specific species of chondroitin sulfate proteoglycan, neurocan, identified with a monoclonal antibody IG2 in the rat cerebrum. Neuroscience 60, 145–157.
Pantazopoulos, H., Woo, T.U.W., Lim, M.P., Lange, N., Berretta, S., 2010. Extracellular matrix-glial abnormalities in the amygdala and entorhinal cortex of subjects diagnosed with schizophrenia. Arch. Gen. Psychiatry 67, 155–166.
Paxinos, G., Franklin, K.B.J., 2012. Paxinos and Franklin's the Mouse Brain in Stereotaxic Coordinates, 4th ed. Academic Press.
Pizzorusso, T., Medini, P., Berardi, N., Chierzi, S., Fawcett, J.W., Maffei, L., 2002. Reactivation of ocular dominance plasticity in the adult visual cortex. Science 8, 1248–1251.
Sadato, N., Yamada, H., Okada, T., Yoshida, M., Hasegawa, T., Matsuki, K.I., Yonekura, Y., Itoh, H., 2004. Age-dependent plasticity in the superior temporal sulcus in deaf humans: a functional MRI study. BMC Neurosci. 5, 56.
Schmalfeldt, M., Bandtlow, C.E., Dours-Zimmermann, M.T., Winterhalter, K.H., Zimmermann, D.R., 2000. Brain derived versican V2 is a potent inhibitor of axonal growth. J. Cell Sci. 113, 807–816.
Schweizer, M., Streit, W.J., Müller, C.M., 1993. Postnatal development and localization of an N-acetylgalactosamine containing glycoconjugate associated with nonpyramidal neurons in cat visual cortex. J. Comp. Neurol. 329, 313–327.
Seeger, G., Brauer, K., Härtig, W., Brückner, G., 1994. Mapping of perineuronal nets in the rat brain stained by colloidal iron hydroxide histochemistry and lectin cytochemistry. Neuroscience 58, 371–388.
Senn, C., Kutsche, M., Saghatelyan, A., Bösl, M.R., Löhler, J., Bartsch, U., Morellini, F., Schachner, M., 2002. Mice deficient for the HNK-1 sulfotransferase show alterations in synaptic efficacy and spatial learning and memory. Mol. Cell Neurosci. 20, 712–729.
Silver, D.J., Silver, J., 2014. Contributions of chondroitin sulfate proteoglycans to neurodevelopment, injury, and cancer. Curr. Opin. Neurobiol. 27, 171–178.
Snow, D.M., Lemmon, V., Carrino, D.A., Caplan, A.I., Silver, J., 1990. Sulfated proteoglycans in astroglial barriers inhibit neurite outgrowth in vitro. Exp. Neurol. 109, 111–130.
Sorg, B.A., Berretta, S., Blacktop, J.M., Fawcett, J.W., Kitagawa, H., Kwok, J.C., Miquel, M., 2016. Casting a wide net: role of perineuronal nets in neural plasticity. J. Neurosci. 36, 11459–11468.
Sur, M., Frost, D.O., Hockfield, S., 1988. Expression of a surface-associated antigen on Y-cells in the cat lateral geniculate nucleus is regulated by visual experience. J. Neurosci. 8, 874–882.
Suttkus, A., Rohn, S., Weigel, S., Glöckner, P., Arendt, T., Morawski, M., 2014. Aggrecan, link protein and tenascin-R are essential components of the perineuronal net to protect neurons against iron-induced oxidative stress. Cell Death. Dis. 13, e1119.
Ueno, H., Suemitsu, S., Okamoto, M., Matsumoto, Y., Ishihara, T., 2017a. Parvalbumin neurons and perineuronal nets in the mouse prefrontal cortex. Neuroscience 343, 115–127.
Ueno, H., Suemitsu, S., Okamoto, M., Matsumoto, Y., Ishihara, T., 2017b. Sensory experience-dependent formation of perineuronal nets and expression of Cat-315 immunoreactive components in the mouse somatosensory cortex. Neuroscience 355, 161–174.
Ueno, H., Suemitsu, S., Murakami, S., Kitamura, N., Wani, K., Okamoto, M., Matsumoto, Y., Ishihara, T., 2017c. Region-specific impairments in parvalbumin interneurons in social isolation-reared mice. Neuroscience 359, 196–208.
Vogt, B.A., 1991. The role of layer I in cortical function. Cereb. Cort., 49–79.
Wegner, F., Härtig, W., Bringmann, A., Grosche, J., Wohlfarth, K., Zuschratter, W., Brückner, G., 2003. Diffuse perineuronal nets and modified pyramidal cells immunoreactive for glutamate and the GABA(A) receptor alpha1 subunit form a unique entity in rat cerebral cortex. Exp. Neurol. 184, 705–714.
Yamada, J., Jinno, S., 2017. Molecular heterogeneity of aggrecan-based perineuronal nets around five subclasses of parvalbumin-expressing neurons in the mouse hippocampus. J. Comp. Neurol. 525, 1234–1249.
Yamada, H., Fredette, B., Shitara, K., Hagihara, K., Miura, R., Ranscht, B., Stallcup, W.B., Yamaguchi, Y., 1997. The brain chondroitin sulfate proteoglycan brevican associates with astrocytes ensheathing cerebellar glomeruli and inhibits neurite outgrowth from granule neurons. J. Neurosci. 17, 7784–7795.
Yamaguchi, Y., 2000. Lecticans: organizers of the brain extracellular matrix. Cell Mol. Life Sci. 57, 276–289.
Yang, S., Cacquevel, M., Saksida, L.M., Bussey, T.J., Schneider, B.L., Aebischer, P., Melani, R., Pizzorusso, T., Fawcett, J.W., Spillantini, M.G., 2015. Perineuronal net digestion with chondroitinase restores memory in mice with tau pathology. Exp. Neurol. 265, 48–58.
Ye, Q., Miao, Q.L., 2013. Experience-dependent development of perineuronal nets and chondroitin sulfate proteoglycan receptors in mouse visual cortex. Matrix Biol. 32, 352–363.